Reactions of Tetrakis(dimethylamide)−Titanium, −Zirconium and −Hafnium with Silanes: Synthesis of Unusual Amide Hydride Complexes and Mechanistic Studies of Titanium−Silicon−Nitride (Ti−Si−N) Formation

Xiaozhan Liu,[†] Zhongzhi Wu,[†] Hu Cai,[†] Yihui Yang,[†] Tianniu Chen,[†] Catherine E. Vallet,[‡] Ray A. Zuhr,[§] David B. Beach,*[,‡] Zhi-Hui Peng,[||] Yun-Dong Wu,*[,||] Thomas E. Concolino,[⊥] Arnold L. Rheingold,*[,⊥] and Ziling Xue*[,†]

Contribution from the Department of Chemistry, University of Tennessee, Knoxville, Tennessee 37996, Chemical and Analytical Sciences Division and Surface Modification and Characterization (SMAC) Research Center, Oak Ridge National Laboratory, Oak Ridge, Tennessee 37831, Department of Chemistry, Hong Kong University of Science and Technology, Hong Kong, and Department of Chemistry and Biochemistry, University of Delaware, Newark, Delaware 19716

Received March 21, 2001

Abstract: $M(NMe_2)_4$ (M = Ti, Zr, Hf) were found to react with $H_2SiR'Ph$ (R′ = H, Me, Ph) to yield H_2, aminosilanes, and black solids. Unusual amide hydride complexes $[(Me_2N)_3M(\mu\text{-}H)(\mu\text{-}NMe_2)_2]_2M$ (M = Zr, **1**; Hf, **2**) were observed to be intermediates and characterized by single-crystal X-ray diffraction. $[(Me_2N)_3M(\mu\text{-}D)(\mu\text{-}NMe_2)_2]_2M$ (**1-*d*$_2$**, **2-*d*$_2$**) were prepared through reactions of $M(NMe_2)_4$ with D_2SiPh_2. Reactions of $(Me_2N)_3ZrSi(SiMe_3)_3$ (**5**) with $H_2SiR'Ph$ were found to give aminosilanes and $(Me_2N)_2Zr(H)Si(SiMe_3)_3$ (**6**). These reactions are reversible through unusual equilibria such as $(Me_2N)_3ZrSi(SiMe_3)_3$ (**5**) + $H_2SiPh_2 \rightleftarrows$ $(Me_2N)_2Zr(H)Si(SiMe_3)_3$ (**6**) + $HSi(NMe_2)Ph_2$. The deuteride ligand in $(Me_2N)_2Zr(D)Si(SiMe_3)_3$ (**6-*d*$_1$**) undergoes H−D exchange with $H_2SiR'Ph$ (R′ = Me, H) to give **6** and HDSiR′Ph. The reaction of $Ti(NMe_2)_4$ with SiH_4 in chemical vapor deposition at 450 °C yielded thin Ti−Si−N ternary films containing TiN and Si_3N_4. $Ti(NMe_2)_4$ reacts with SiH_4 at 23 °C to give H_2, $HSi(NMe_2)_3$, and a black solid. $HNMe_2$ was not detected in this reaction. The reaction mixture, upon heating, gave TiN and Si_3N_4 powders. Analyses and reactivities of the black solid revealed that it contained −H and unreacted $-NMe_2$ ligands but no silicon-containing ligand. Ab initio quantum chemical calculations of the reactions of $Ti(NR_2)_4$ (R = Me, H) with SiH_4 indicated that the formation of aminosilanes and $HTi(NR_2)_3$ was favored. These calculations also showed that $HTi(NH_2)_3$ (**3b**) reacted with SiH_4 or H_3Si-NH_2 in the following step to give $H_2Ti(NH_2)_2$ (**4b**) and aminosilanes. The results in the current studies indicated that the role of SiH_4 in its reaction with $Ti(NMe_2)_4$ was mainly to remove amide ligands as $HSi(NMe_2)_3$. The removal of amide ligands is incomplete, and the reaction thus yielded "═Ti(H)(NMe_2)" as the black solid. Subsequent heating of the black solid and $HSi(NMe_2)_3$ may then yield TiN and Si_3N_4, respectively, as the Ti−Si−N materials.

Introduction

Transition metal amide ligands are known to react with proton- or hydride-containing compounds to yield amines (H−NR_2).[1] Such reactions include those with H_2O, $HSnPh_3$,[2] and a silane $HSi(C_6F_5)_3$.[3] Thus far, to our knowledge, there has been only one report about a reaction between a late-transition-metal d^8 amide $Cp^*Ni(PEt_3)NH(CH_2Ph)$ and $HSiMe_3$ to give a hydride $Cp^*Ni(PEt_3)H$.[4] Recent reports[5−10] of formation of Ti−Si−N ternary materials from the reactions of $Ti(NR_2)_4$, SiH_4, and NH_3 as barrier materials between Cu and Si in integrated circuits prompted us to investigate the nature of the reactions between amide ligands (M−NR_2) and silanes (H−Si).

Copper has been used as a new generation of interconnection metal in Si-based integrated microelectronic devices.[11] Materials as diffusion barriers[12,13] between the Cu layer and semiconductor Si are of intense current interest to prevent solid-state reactions between Cu and Si (to form copper silicides $CuSi_n$)[14,15] and the degradation of the devices. Titanium nitride TiN has been

[†] University of Tennessee.
[‡] Chemical and Analytical Sciences Division, Oak Ridge National Laboratory.
[§] Surface Modification and Characterization (SMAC) Research Center, Oak Ridge National Laboratory.
[||] Hong Kong University of Science and Technology.
[⊥] University of Delaware.

(1) (a) Lappert, M. F.; Power, P. P.; Sanger, A. R.; Srivastava, R. C. *Metal and Metalloid Amides*; Ellis Horwood: Chichester, U.K., 1980. (b) Chisholm, M. H.; Rothwell, I. P. In *Comprehensive Coordination Chemistry*; Wilkinson, G., Gillard, R. D., McCleverty, J. A. Eds.; Pergamon: New York, 1987; Vol. 2. (c) Kempe, R. *Angew. Chem. Int. Ed.* **2000**, *39*, 468.

(2) $M(NR_2)_4 + 4HSnPh_3 \rightarrow M(SnPh_3)_4 + 4HNR_2$ (M = Ti, R = Me; M = Zr, R = Et). Creemers, H. M. J. C.; Verbeek, F.; Noltes, J. G. *J. Organomet. Chem.* **1968**, *15*, 125. A radical mechanism here is also possible.

(3) $M(NR_2)_2 + 2HSiR'_3 \rightarrow M(SiR'_3)_2 + 2HNR_2$ (M = Cd, Hg; R = $SiMe_3$; R′ = C_6F_5). Kalinina, G. S.; Petrov, B. I.; Kruglaya, O. A.; Vyazankin, N. S. *J. Gen. Chem. USSR (Engl. Transl.)* **1972**, *42*, 144.

(4) Holland, P. L.; Andersen, R. A.; Bergman, R. G.; Huang, J.; Nolan, S. P. *J. Am. Chem. Soc.* **1997**, *119*, 12800.

(5) (a) *The Chemistry of Metal CVD*; Kodas, T. T., Hampden-Smith, M. J., Eds.; VCH: Weinheim, Germany, 1994. (b) Winter, C. H. *Aldrichimica Acta* **2000**, *33*, 3.

(6) Raaijmakers, I. J. *Thin Solid Films* **1994**, *247*, 85.

(7) (a) Reid, J. S.; Sun, X.; Kolawa, E.; Nicolet, M.-A. *IEEE Electron Device Lett.* **1994**, *15*, 298. (b) Reid, J. S.; Kolawa, E.; Garland, C. M.; Nicolet, M.-A.; Cardone, F.; Gupta, D.; Ruiz, R. P. *J. Appl. Phys.* **1996**, *79*, 1109. (c) Custer, J. S.; Smith, P. M.; Jones, R. V.; Maverick, A. W.; Roberts, D. A.; Norman, J. A. T.; Hochberg, A. K. *Mater. Res. Soc. Symp. Proc.* **1996**, *427* (*Advanced Metallization for Future ULSI*; Tu, K. N., Mayer, J. W., Poate, J. M., Chen, L. J., Eds.), 343.

10.1021/ja010744s CCC: $20.00 © 2001 American Chemical Society
Published on Web 07/20/2001

studied as such a diffusion-barrier material.[16] TiN films in these diffusion barriers are usually polycrystalline with grain boundaries between TiN crystals, and these grain boundaries often lead to diffusion between Cu and Si layers.[6,7a,8a,13,17] The barrier properties of TiN films may thus be inadequate. One of the most promising barrier materials for copper interconnect is amorphous ternary alloy Ti−Si−N.[5−10,15] The absence of grain boundaries in amorphous Ti−Si−N significantly reduces the likelihood of diffusion between Cu and Si layers, and Ti−Si−N ternary phase has demonstrated superior diffusion barrier properties.[5b,7−8]

Chemical vapor deposition (CVD) of Ti−Si−N thin films is thus of intense current interest.[6−10,18−19] Raajimaker first reported the CVD of Ti−Si−N thin films from reactions of Ti(NEt$_2$)$_4$ with NH_3 and SiH_4 in 1994.[6] Li and co-workers developed a plasma-enhanced CVD process for the deposition of Ti−Si−N at 560 °C.[18] Nicolet, Smith, and co-workers have studied various CVD processes with Ti(NEt$_2$)$_4$, SiH_4, and NH_3 as precursors to give Ti−Si−N ternary films.[7,8] Detailed analyses showed that these Ti−Si−N ternary films are mixtures of TiN and Si_3N_4; The compositions of these films were near or above the TiN and Si_3N_4 tie-lines in Ti−N−Si ternary phase diagram,[7c,8] and there were no $TiSi_n$ phases in the films. The mechanism of such reactions is yet not clear, but it is reasonable to assume that the stoichiometry (ratios of M:Si:N) in the M−Si−N ternary products is determined to a large extent by the reaction mechanism. A key question is why the reactions of Ti(NEt$_2$)$_4$ with SiH_4 and NH_3 gave TiN and Si_3N_4 in the Ti−Si−N ternary phases.[8b]

The probable role of NH_3 in these reactions is that it undergoes transamination with Ti−NMe$_2$.[16,20] We have thus focused our studies on the mechanistic pathways in the reactions of d^0 M(NMe$_2$)$_4$ (M = Ti, Zr, Hf) with silanes. We were surprised to find that these reactions gave aminosilanes, H_2, and amide hydrides such as unusual trinuclear complexes [(Me$_2$N)$_3$M(*μ*-H)(*μ*-NMe$_2$)$_2$]$_2$M (M = Zr, **1**; Hf, **2**). The reaction between Ti(NMe$_2$)$_4$ and SiH_4 in chemical vapor decomposition (CVD) was found to yield Ti−Si−N ternary films containing Si_3N_4 and TiN. We report here our experimental and theoretical studies of these reactions and mechanistic pathways in the reactions between Ti(NMe$_2$)$_4$ and SiH_4 to give Ti−Si−N ternary materials.[21]

Experimental Section

General Procedures. All manipulations, unless noted, were performed under a dry N_2 atmosphere with the use of the Schlenk techniques.[22] All solvents were purified by distillation from K/benzophenone ketyl. Benzene-d_6, toluene-d_8, H_3SiPh (Aldrich), H_2SiPh_2 (Aldrich), and $H_2SiMePh$ (Gelest) were dried over molecular sieves and stored under N_2. Unless noted, SiH_4 (5% in Ar, Air Products) was used. M(NMe$_2$)$_4$ (M = Ti,[23] Zr,[23,24] Hf[23]) and (Me$_2$N)$_3$ZrSi(SiMe$_3$)$_3$ (**5**)[25] were prepared by the literature procedures. D_2SiPh_2, D_3SiPh, and $D_2SiMePh$ were prepared by reactions of $LiAlD_4$ with Ph_2SiCl_2, Cl_3SiPh, and $Cl_2SiMePh$, respectively.[26] Ph_2SiCl_2 (Gelest) was distilled prior to use. HNMe$_2$ gas was generated by bubbling N_2 through a 40 wt % aqueous solution of HNMe$_2$ (Aldrich), dried over a KOH-filled column, and condensed as a liquid at −78 °C. DCl (37 wt % solution in D_2O, Aldrich) was diluted with D_2O to form a 1 M solution.

^{1}H, ^{2}H, ^{13}C{^{1}H}, and ^{29}Si{^{1}H} (DEPT) NMR spectra were recorded on a Bruker AC-250 or AMX-400 spectrometer. They were referenced to residual protons, external toluene-d_8, solvent, and SiMe$_4$, respectively. The assignments of aminosilanes were based on reported NMR and standard MS.[21] FT-IR spectra of KBr pellets and Raman spectra were recorded on a Bio-Rad FTS-60A spectrometer and a Dilor X-Y micro-Raman spectrometer, respectively. Mass spectra (MS) were recorded on a VG ZAB-EQ hybrid high-performance mass spectrometer (ionization voltage of 70 eV). A Hewlett-Packard 6890 gas chromatograph (GC) with a 5793 mass selective (MS) detector (MSD) was used to obtain GC/MS data. Elemental analyses were performed by E+R Microanalytical Laboratory, Corona, New York.

Preparation of [(Me$_2$N)$_3$Zr(*μ*-H)(*μ*-NMe$_2$)$_2$]$_2$Zr (1). To a solution of Zr(NMe$_2$)$_4$ (0.32 g, 1.2 mmol) in Et$_2$O (10 mL) was added H_2SiPh_2 (0.22 mL, 1.2 mmol) in Et$_2$O (5 mL). After the addition, the solution was cooled to −40 °C immediately, and the solvent was removed in vacuo. The yellow residue was washed with cold Et$_2$O several times to remove organic products. Recrystallization from cold Et$_2$O afforded 0.11 g (0.15 mmol) of **1** as yellow blocks [38% yield based on Zr(NMe$_2$)$_4$]. ^{1}H and ^{13}C NMR, HMQC, and NOSEY were used in structure assignments. Data for **1**: ^{1}H NMR (benzene-d_6, 250.1 MHz, 23 °C) δ 5.21 (s, 2H, Zr-*H*), 2.98 (s, 60H, N*Me$_2$*); ^{13}C{^{1}H} (benzene-d_6, 62.9 MHz, 23 °C) δ 44.54 (N*Me$_2$*). ^{1}H NMR (toluene-d_8, 400.1 MHz, −70 °C) δ 5.11 (s, 2H, Zr-*H*), 3.24 (s, 36H, terminal N*Me$_2$*), 3.05 (s, 6H, *μ*-N*Me$_2$*), 2.60 (s, 6H, *μ*-N*Me$_2$*), 2.58 (s, 6H, *μ*-N*Me$_2$*), 2.46 (s, 6H, *μ*-N*Me$_2$*); ^{13}C{^{1}H} (toluene-d_8, 100.6 MHz, −70 °C) δ 45.32 (terminal N*Me$_2$*), 43.25 (*μ*-N*Me$_2$*), 43.06 (*μ*-N*Me$_2$*), 42.14 (*μ*-N*Me$_2$*). Anal. Calcd for $C_{20}H_{62}N_{10}Zr_3$: C, 33.53; H, 8.72. Found: C, 33.20; H, 8.34. **1** was similarly prepared from the reactions of Zr-

(8) (a) Smith, P. M.; Custer, J. S. *Appl. Phys. Lett.* **1997**, *70*, 3116. (b) Custer, J. S.; Smith, P. M.; Fleming, J. G.; Roherty-Osmun, E. *ACS Symp. Ser*. **1999**, *727* (*Inorganic Materials Synthesis*; Winter, C. H., Hoffman, D. M., Eds.), 86.

(9) (a) Min, J.-S.; Park, J.-S.; Park, H.-S.; Kang, S.-W. *J. Electrochem. Soc.* **2000**, *147*, 3868. (b) Eisenbraun, E.; Upham, A.; Dash, R.; Zeng, W.-X.; Hoefnagels, J.; Lane, S.; Anjum, D.; Dovidenko, K.; Kaloyeros, A.; Arkles, B.; Sullivan, J. J. *J. Vac. Sci. Technol., B* **2000**, *18*, 2011. (c) Le Brizoual, L.; Guilet, S.; Lemperiere, G.; Granier, A.; Coulon, N.; Lancin, M.; Turban, G. *Microelectron. Eng.* **2000**, *50*, 509. (d) No, J.-T.; O, J.-H.; Lee, C.-M. *Mater. Chem. Phys.* **2000**, *63*, 44. (e) Park, J.-S.; Sohn, D. K.; Lee, B. H.; Bae, J.-U.; Byun, J. S.; Park, J. W. *J. Electrochem. Soc.* **1999**, *146*, 1579. (f) Zhang, J.-M.; Venkatraman, R.; Wilson, T.; Fiordalice, R.; Gregory, R.; Weitzman, E. *Mater. Res. Soc. Symp. Proc*. **1998**, *514*, 513. (g) Asai, K.; Sugahara, H.; Matsuoka, Y.; Tokumitsu, M. *J. Vac. Sci. Technol.* **1988**, *B6*, 1526.

(10) Doan, T. T.; Sandhu, G. S. U.S. Patent Nos. 5,278,100, 1994; 5,-376,405, 1994; 5,252,518, 1993.

(11) Jain, A.; Chi, K. M.; Shin, H. K.; Farkas, D. J.; Kodas, T. T.; Hampden-Smith, M. J. *Semicond. Int.* **1993**, *16*, 128.

(12) Mayer, J. W.; Lau, S. S. *Electronic Materials Science: For Interconnection Circuits in Si and GaAs*; Macmillan: New York, 1990.

(13) Nicolet, M.-A. *Thin Solid Films* **1978**, *52*, 415.

(14) Li, J.; Mayer, J. W. *MRS Bull.* **1993**, *18(6)*, 52.

(15) Kolawa, E.; Pokela, P. J.; Reid, J. S.; Chen, J. S.; Ruiz, R. P.; Nicolet, M.-A. *IEEE Electron Device Lett.* **1991**, *12*, 321.

(16) (a) Fix, R.; Gordon, R. G.; Hoffman, D. M. *Chem. Mater*. **1991**, *3*, 1138. (b) Beaudoin, M.; Scott, S. L. *Organometallics* **2001**, *20*, 237.

(17) Eizenberg, M.; Littau, K.; Ghanayem, S.; Mak, A.; Maeda, Y.; Chang, M.; Sinha, A. K. *Appl. Phys. Lett.* **1994**, *65*, 2416.

(18) Li, S.; Shi, Y.; Peng, H. *Plasma Chem. Plasma Process.* **1992**, *12*, 287.

(19) Amato-Wierda, C. C.; Norton, E. T., Jr.; Wierda, D. A. *Chem. Mater.* **1999**, *11*, 2775.

(20) (a) Weiller, B. H. *J. Am. Chem. Soc.* **1996**, *118*, 4975. (b) Cundari, T. R.; Morse, J. M. *Chem. Mater.* **1996**, *8*, 189.

(21) Preliminary results have been reported. Liu, X.; Wu, Z.; Peng, Z.; Wu, Y.; Xue, Z. *J. Am. Chem. Soc.* **1999**, *121*, 5350 and 8969.

(22) See Supporting Information for details.

(23) Bradley, D. C.; Thomas, I. M. *J. Chem. Soc.* **1960**, 3857.

(24) (a) Chisholm, M. H.; Hammond, C. E.; Huffman, J. C. *Polyhedron* **1988**, *7*, 2515. (b) Diamond, G. M.; Jordan, R. F.; Petersen, J. L. *J. Am. Chem. Soc.* **1996**, *118*, 8024.

(25) Wu, Z.; Diminnie, J. B.; Xue, Z. *Inorg. Chem.* **1998**, *37*, 6366. For other related d^0 Cp-free silyl complexes, see: Xue, Z.; Li, L.; Hoyt, L. K.; Diminnie, J. B.; Pollitte, J. L. *J. Am. Chem. Soc.* **1994**, *116*, 2169. Li, L.; Diminnie, J. B.; Liu, X.; Pollitte, J. L.; Xue, Z. *Organometallics* **1996**, *15*, 3520. McAlexander, L. H.; Hung, M.; Li, L.; Diminnie, J. B.; Xue, Z.; Yap, G. P. A.; Rheingold, A. L. *Organometallics* **1996**, *15*, 5231. Wu, Z.; Diminnie, J. B.; Xue, Z. *Organometallics* **1998**, *17*, 2917. Liu, X.; Li, L.; Diminnie, J. B.; Yap, G. P. A.; Rheingold, A. L.; Xue, Z. *Organometallics* **1998**, *17*, 4597. Chen, T.; Wu, Z.; Li, L.; Sorasaenee, K. R.; Diminnie, J. B.; Pan, H.; Guzei, I. A.; Rheingold, A. L.; Xue, Z. *J. Am. Chem. Soc.* **1998**, *120*, 13519. Choi, S.-H.; Lin, Z.; Xue, Z. *Organometallics* **1999**, *18*, 5488. Wu, Z.; Xue, Z. *Organometallics* **2000**, *19*, 4191. Xue, Z. *Comments Inorg. Chem.* **1996**, *18*, 223.

(26) Gilman, H.; Dunn, G. E. *J. Am. Chem. Soc.* **1951**, *73*, 3404.

(NMe$_2$)$_4$ with H$_3$SiPh, H$_2$SiMePh, and HSi(NMe$_2$)Ph$_2$. Variable-temperature NMR studies of **1** were conducted with 0.053 g (0.074 mmol) of **1** and 0.2 mg of 4,4′-dimethylbiphenyl (an internal standard) in toluene-d_8 between −80 and 0 °C.

Preparation of [(Me$_2$N)$_3$Hf(μ-H)(μ-NMe$_2$)$_2$]$_2$Hf (2). To a solution of Hf(NMe$_2$)$_4$ (1.015 g, 2.861 mmol) in Et$_2$O (10 mL) was added dropwise 0.53 mL of H$_2$SiPh$_2$ (0.53 g, 3.0 mmol) in Et$_2$O. After the addition was complete, the mixture was stirred for 10 min, and then cooled to −35 °C. The volatile products were removed under vacuum, and the colorless solid was washed with cold Et$_2$O (−50 °C, 15 mL) three times to extract organic products. The solid was then dissolved in Et$_2$O, and the solution was cooled to −30 °C, yielding 0.55 g of colorless crystals of **2** [59% yield based on Hf(NMe$_2$)$_4$]. ^{1}H and ^{13}C{^{1}H} NMR and HMQC were used in structure assignments. Data for **2**: ^{1}H NMR (benzene-d_6, 250.1 MHz, 23 °C) δ 9.87 (s, 2H, Hf-*H*), 3.01 (s, 60H, N*Me*$_2$); ^{13}C{^{1}H} (benzene-d_6, 62.9 MHz, 23 °C) δ 44.25 (N*Me*$_2$). Anal. Calcd for C$_{20}$H$_{62}$N$_{10}$Hf$_3$: C, 24.56; H, 6.39. Found: C, 24.22; H, 6.37. **2** was similarly prepared from the reactions of Hf(NMe$_2$)$_4$ with H$_3$SiPh, H$_2$SiMePh, and HSi(NMe$_2$)Ph$_2$.

Preparation of [(Me$_2$N)$_3$M(μ-D)(μ-NMe$_2$)$_2$]$_2$M (M = Zr, 1-*d*$_2$; M = Hf, 2-*d*$_2$). To a solution of Zr(NMe$_2$)$_4$ (0.0423 g, 0.158 mmol) in toluene was added D$_2$SiPh$_2$ (0.029 mL, 0.16 mmol). The color changed from pale yellow to intense lemon in the formation of **1-*d*$_2$**. ^{2}H (toluene, 61.4 MHz, 23 °C) of **1-*d*$_2$** δ 5.24 (s, 2D, Zr-*D*). The hafnium analogue **2-*d*$_2$** was prepared similarly. ^{2}H (toluene, 61.4 MHz, 23 °C) of **2-*d*$_2$** δ 9.98 (s, 2D, Hf-*D*).

X-ray Crystal Structure Determination of 1 and 2. A yellow crystal of **1** was selected in Paratone oil and mounted on a Siemens R3m/V diffractometer (Mo Kα radiation, 0.71073 Å) under a N$_2$ stream at −100 °C. The unit cell parameters and orientation matrix were determined from a least-squares fit of 30 reflections obtained from a rotation photograph and an automatic peak search routine. All non-hydrogen atoms were refined anisotropically. The two hydride atoms were located and refined isotopically, and the remaining H atoms were treated as idealized contributions. All calculations were performed using the SHLEXTL (5.10) program library.[27a]

The single-crystal X-ray diffraction experiment for **2** was performed on a Siemens P4/CCD diffractometer. Systematic absences and diffraction symmetry were uniquely consistent for the assigned space group. The structure was solved by direct methods, completed by subsequent difference Fourier syntheses, and refined by a full-matrix, least-squares procedure. All non-H atoms were refined with anisotropic coefficients, and all H atoms, except as noted below, were treated as idealized contributions. An empirical absorption correction was applied to the data using the program DIFABS.[27b] The bridging hydrides could not be located from the difference map and were ignored in the refinement, but not in the global parameters. All calculations were performed using the SHLEXTL (5.10) program library.[27a]

Reaction of (Me$_2$N)$_3$ZrSi(SiMe$_3$)$_3$ (5) with H$_2$SiPh$_2$. H$_2$SiPh$_2$ (47.2 mg, 0.256 mmol) was added to **5** (30 mg, 0.064 mmol) in benzene-d_6 at 23 °C. The color of the solution gradually changed from pale yellow to red. (Me$_2$N)$_2$Zr(H)Si(SiMe$_3$)$_3$ (**6**) and HSi(NMe$_2$)Ph$_2$ were observed in ^{1}H NMR, and the reaction was found to reach equilibrium. Two separate ^{1}H NMR samples were used to measure the equilibrium constant for this reaction at 0 °C. **6** was found to slowly decompose to HSi(SiMe$_3$)$_3$ and unidentified precipitates. Reactions of **5** with H$_2$SiMePh and H$_3$SiPh give **6**, and HSi(NMe$_2$)MePh and H$_2$Si(NMe$_2$)Ph, respectively. Data for **6**: ^{1}H NMR (benzene-d_6, 250.1 MHz, 23 °C) δ 5.68 (s, 1H, Zr*H*), 2.83 (s, 12H, N*Me*$_2$), 0.40 (s, 27H, Si*Me*$_3$); ^{13}C{^{1}H} (benzene-d_6, 62.9 MHz, 23 °C) δ 40.98 (N*Me*$_2$), 5.67 (Si*Me*$_3$); ^{29}Si{^{1}H} NMR (benzene-d_6, 79.5 MHz, 23 °C) δ −5.2 (*Si*Me$_3$), −126.1 (*Si*SiMe$_3$).

Confirmation of the Equilibrium: (Me$_2$N)$_3$ZrSi(SiMe$_3$)$_3$ (5) + H$_2$SiMePh ⇄ (Me$_2$N)$_2$Zr(H)Si(SiMe$_3$)$_3$ (6) + HSi(NMe$_2$)MePh. H$_2$SiMePh (7.8 mg, 0.064 mmol) was added to **5** (30 mg, 0.064 mmol) in benzene-d_6 at 23 °C. Once the reaction reached equilibrium (as monitored by NMR), HSi(NMe$_2$)Ph$_2$ (14.5 mg, 0.064 mmol) was added to the reaction mixture. NMR spectra of the reaction mixture showed the formation of H$_2$SiPh$_2$.

Hydrogen Exchange between 6-*d*$_1$ and H$_2$SiMePh. (Me$_2$N)$_3$ZrSi(SiMe$_3$)$_3$ (**5**, 30 mg) and D$_2$SiMePh (25 mg) were mixed in benzene-d_6 at 23 °C to yield (Me$_2$N)$_2$Zr(D)Si(SiMe$_3$)$_3$ (**6-*d*$_1$**) and DSi(NMe$_2$)MePh. After 10 min, 25 mg of H$_2$SiMePh was added. ^{1}H NMR of the solution showed the formation of HDSiMePh, (Me$_2$N)$_2$Zr(H)Si(SiMe$_3$)$_3$ (**6**), and HSi(NMe$_2$)MePh. A similar H−D exchange was observed between **6-*d*$_1$**, prepared from **5** and D$_3$SiPh, and H$_3$SiPh. In a control experiment, D$_2$SiMePh and H$_2$SiMePh were dissolved in benzene-d_6 at 23 °C. The ^{1}H NMR of this control solution did not show the formation of HDSiMePh.

Reaction of Zr(NMe$_2$)$_4$ with H$_2$SiPh$_2$ in the Presence of HNMe$_2$. H$_2$SiPh$_2$ (0.115 mL, 0.621 mmol) was added to Zr(NMe$_2$)$_4$ (27.7 mg, 0.104 mmol) and 4,4′-dimethylbiphenyl (an internal standard) in benzene-d_6 in an NMR tube (Tube A). The mixture was then immediately cooled to −70 °C. HNMe$_2$ (0.0774 mmol) was vacuum transferred to the NMR tube. The mixture was then warmed to 23 °C. As in the reaction without external HNMe$_2$, the formation of HSi(NMe$_2$)Ph$_2$ and H$_2$ was observed in NMR, and the peak of Zr(NMe$_2$)$_4$ disappeared in ca. 5 min.

Three new peaks in ^{1}H NMR [2.21 (s, C*H*$_3$), 2.19 (s, C*H*$_3$) and 0.18 (br, *H*-N) ppm] and one new peak in ^{13}C{^{1}H} NMR (38.8 ppm) were observed, respectively, in the reaction mixture. [In comparison HNMe$_2$ in a benzene-d_6 solution of H$_2$SiPh$_2$ was found to be at 2.20 ppm (s, 6H, C*H*$_3$) and 0.33 ppm (br, 1H, *H*-N) in ^{1}H NMR and 38.9 ppm in ^{13}C{^{1}H} NMR.] The integrals of these two peaks in ^{1}H NMR decreased by 10% in 6 h after the addition of HNMe$_2$.

The nature of the chemical species giving these new NMR peaks was investigated. A portion of the volatile products in the reaction mixture was vacuum transferred to another NMR tube (Tube B) containing benzene-d_6 and the internal standard. The integrals of these two ^{1}H NMR peaks in the remaining mixture (Tube A) were found to have decreased, and HNMe$_2$ was observed in Tube B. The volatile products in Tube B were then transferred back to Tube A, and the integrals of these two ^{1}H NMR peaks were found to have increased. Although we do not know the nature of the chemical species that give(s) these new NMR peaks, they are perhaps HNMe$_2$ coordinated to colloidal Zr species. The observation that these two new peaks decreased by 10% in 6 h indicated that the reaction of HNMe$_2$ with H$_2$SiPh$_2$, if occurring in the reaction mixture, was much slower than that of Zr(NMe$_2$)$_4$ with H$_2$SiPh$_2$.

Reactions of M(NMe$_2$)$_4$ (M = Ti, Zr, Hf) with Silanes in Solution and the Analysis of the Solid Product. One equivalent of H$_2$SiR′Ph (R′ = H, Me, Ph) was added to M(NMe$_2$)$_4$ in benzene-d_6. The solution turned dark yellow immediately. When more than 1 equiv of the silane was used, the solution turned black with gas evolution. The organic products were identified by NMR as HSi(NMe$_2$)R′Ph. The black solid product from the reaction of Ti(NMe$_2$) with the phenylsilanes was further analyzed. Ti(NMe$_2$)$_4$ (0.448 g, 2.00 mmol) with H$_2$SiPh$_2$ (1.475 g, 8.00 mmol) were mixed in hexanes (30 mL) and stirred overnight at 23 °C. The black solid was isolated by filtration, washed with Et$_2$O six times, and then dried under vacuum. The black solid was then added to DCl in D$_2$O (1 M, excess) frozen in a Schlenk flask by liquid N$_2$. The flask was then evacuated, closed, and then warmed to 23 °C. Once bubbling of gas stopped, the flask was opened to another previously evacuated tube. The hydrogen gas in this tube was analyzed by MS and shown to contain H$_2$, HD, and D$_2$ in 9:100:33 ratios. In separate experiments, the black solids were similarly prepared from the reactions of Ti(NMe$_2$)$_4$ with H$_2$SiR′Ph (R′ = H, Me, Ph), washed with hexanes six times, and dried under vacuum. An IR analysis of the black solids showed *no* presence of aminosilanes, indicating that the hydrogen gas is the product of the reaction of the black solids with DCl/D$_2$O. The black solids were then treated with DCl in D$_2$O (1 M, excess). The analysis of the products by GC/MS showed the presence of DNMe$_2$, but no H$_2$SiR′Ph, HDSiR′Ph, or D$_2$SiR′Ph.

In another experiment, Ti(NMe$_2$)$_4$ liquid (0.0116 g, 0.0517 mmol) in toluene-d_8 was evacuated at −196 °C, and excess SiH$_4$ was introduced. The system was slowly warmed to 23 °C. H$_2$, H$_2$Si(NMe$_2$)$_2$, and HSi(NMe$_2$)$_3$ were identified as the products by ^{1}H NMR.

Reactions of Liquid Ti(NMe$_2$)$_4$ and Solid Zr(NMe$_2$)$_4$ with SiH$_4$ and the Preparation of Powders 7 and 8. A scheme of a reaction manifold is given in the Supporting Information.[22] The system (base

(27) (a) Sheldrick, G. M. Bruker AXS, Inc., Madison, WI. (b) Walker, N.; Stuart, D. *Acta Crystallogr., Sect. A* **1983**, *A39*, 158.

pressure of 10^{-5} Torr), consists of an oil diffusion pump, a Schlenk-type quartz tube fitted into a furnace, stainless steel tubing, Cajon O-ring-type fittings, and a SiH_4 tank. SiH_4 was introduced as a flowing gas and was exhausted slowly into a fume hood after passing through an aqueous KOH solution.

$Ti(NMe_2)_4$ (0.067 g, 0.30 mmol) in the tube was cooled to −196 °C and the system was evacuated. SiH_4 was then introduced at 23 °C. The color of the liquid turned black with gas evolution and precipitation of a black solid. When gas evolution had ceased, the system was evacuated overnight. The volatile products collected at −196 °C were found to contain $HSi(NMe_2)_3$. SiH_4 was then reintroduced. The procedure was repeated five times. At this point, no gas evolved when new SiH_4 was introduced. At −77 °C, the tube was evacuated, sealed, and heated to 1090 °C for ca. 60 h. It was cooled afterward to 350 °C at 0.05 °C/min, and then in air to 23 °C to give powder **7**. Powder **8** was prepared by this process as well except that the tube was heated at 700 °C. The reaction of solid $Zr(NMe_2)_4$ with excess SiH_4 was similarly conducted to identify organic products.[22]

Thin Film Deposition in an Ultrahigh-Vacuum (UHV) CVD Chamber.[29] A scheme of the CVD chamber is given in the Supporting Information.[22,29] A Si(100) wafer as substrate was placed in the middle heating zone through a loading lock and heated at 448−450 °C. The system was evacuated and purged for 30 min around 400 °C before each deposition. Under these conditions, analyses of the ultrahigh-purity Ar outflow by mass spectrometry showed that it contained no O_2. $Ti(NMe_2)_4$ was evacuated at −193 °C, and then carried by Ar to the chamber at 450 sccm (standard cubic centimeter per minute) with delivery inlet at 264 °C. SiH_4 (Matheson, ULSI grade, 99.999+%) was introduced into the chamber through a separate inlet at 140 sccm. The deposition chamber pressures were 5.0 Torr. After the deposition, film **9** was annealed to 750 °C under vacuum for 2 h and then allowed to cool slowly in the reactor under vacuum.

Powder and Thin Film Analysis. Powder X-ray diffraction (XRD) analyses were conducted on a Phillips X-ray diffractometer. Powder **7** was analyzed by XRD. Energy dispersive spectroscopy (EDS) of powder **8** was conducted on a Hitachi S-800 scanning electron microscope. Rutherford backscattering spectroscopy (RBS)[28] of film **9** was obtained using 2.3 MeV $^4He^+$ with a standard silicon surface barrier detector placed at ∼160° scattering angle at Surface Modification and Characterization (SMAC) research center at Oak Ridge National Laboratory. X-ray photoelectron spectroscopy (XPS) analyses of powder **8** were performed on a V. G. Scientific 5000 system. XPS analyses of film **9** were carried out on a Perkin-Elmer ESCA/SAM system with a PE Φ 32-095 model X-ray source at 20 mA and 15 kV. The electron-energy analyzer was calibrated to the Au $4f_{7/2}$ line at 84 eV. The Mg Kα excitation (1253.6 eV) from an Al/Mg dual anode (PE Φ 04−500 model) was used to excite photoemission, and photoelectrons were detected at an angle of 40° with respect to the plane of the surface. Sputtering was done with a differentially pumped ion gun (PE Φ 04-300 model) providing an Ar^+ current of 1 mA at 3 keV, rastered over an area of 3×3 mm^2 with sputter rate of 30 Å/min. Base pressure in the XPS chamber was 10^{-9} Torr, while the maximum pressure in the chamber during sputtering was 4.0×10^{-7} Torr. The electron-energy analyzer was set for a pass energy of 178 eV for general survey mode. The composition was determined according to the XPS multiplex spectrum. The depth profile of film **9** was obtained at the base pressure of 10^{-7} Torr with the Ar^+ gun on.

Calculation Method. The calculation method was similar to those reported earlier.[30] Calculations were carried out with the GAUSSIAN 94 program.[31] Geometries were initially optimized by the HF/3-21G method. Harmonic vibration frequencies were calculated for these geometries. The geometries were further optimized with the HF/HW3 method. Energies were evaluated with the MP2/HW3 method and with the HF/HW3 geometries.

Scheme 1. Possible Pathways in the First Step in the Reactions between Metal Amides and Silanes

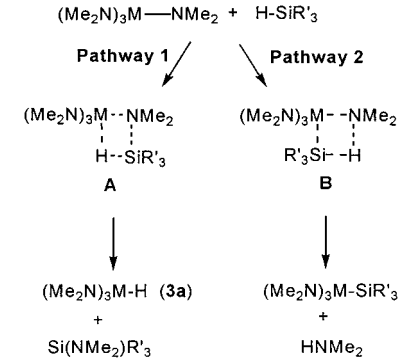

Results and Discussion

Two possible pathways in the first step of the reaction of $M(NMe_2)_4$ with silane are shown in Scheme 1. If the reaction occurs through Pathway 1, aminosilane $Si(NMe_2)R'_3$ and hydride $HM(NMe_2)_3$ (**3a**) are expected. If Pathway 2 is the preferred process, dimethylamine $HNMe_2$ and a silyl complex $(Me_2N)_3M\text{-}SiR'_3$ are the major products.

Reactions of $M(NMe_2)_4$ (M = Ti, Zr, Hf) with Silanes and Preparation of Amide Hydride Complexes $[(Me_2N)_3M(\mu\text{-}H)(\mu\text{-}NMe_2)_2]_2M$ (M = Zr, 1; Hf, 2). When $M(NMe_2)_4$ (M = Ti, Zr) were exposed to excess SiH_4 (5% in Ar) or $H_2SiR'Ph$ (R′ = H, Ph, Me) at 23 °C, fast reactions were observed, yielding aminosilanes [$HSi(NMe_2)_3$, $HSi(NMe_2)_2Ph$, $HSi(NMe_2)Ph_2$, and $HSi(NMe_2)MePh$, respectively], H_2, and black solids. No $HNMe_2$ was detected. The formation of aminosilanes was found to be stepwise: $H_2Si(NMe_2)_2$ and $H_2Si(NMe_2)Ph$ were observed as intermediates when SiH_4 and H_3SiPh were used, respectively. Similar reactions were observed between $Hf(NMe_2)_4$ and $H_2SiR'Ph$. In the investigations here, the black solids (without heating) were studied directly by chemical and spectroscopic methods.

In the reactions of $Ti(NMe_2)_4$ with these silanes at room temperature, nearly 95% of the amide ligands were found to transfer from the Ti center to the silanes to give aminosilanes. In the reactions of its Zr and Hf analogues $M(NMe_2)_4$ (M = Zr, Hf) with phenylsilanes at room temperature, the aminosilanes products accounted for only about 45% of the amide ligands in $M(NMe_2)_4$. This suggested that many amide ligands were left on the metal.

In contrast to the vigorous reactions between $Ti(NMe_2)_4$ and SiH_4 or phenylsilanes, no reactions were observed between this amide complex and alkylsilanes such as $H_2SiBu^t_2$ and $HSiEt_3$ in benzene-d_6, even at elevated temperatures (up to 70 °C). At elevated temperatures, only the decomposition of the metal complexes was observed. It is not clear why there were no reactions between the alkylsilanes and $Ti(NMe_2)_4$.

The insoluble black solids were washed several times to remove aminosilanes and dried under vacuum before they were used in the following analyses and reactions. IR of the black

(28) (a) Feldman, L. C.; Mayer, J. W. *Fundamentals of Surface and Thin Film Analysis*; North-Holland: New York, 1986. (b) Russell, T. P. *Annu. Rev. Mater. Sci.* **1991**, *21*, 249. (c) Watts, J. F. *An Introduction to Surface Analysis by Electron Spectroscopy*; Oxford University Press: London, 1990.

(29) For a scheme and description of a similar CVD chamber, see Kouvetakis, J.; Beach, D. B. *Chem. Mater.* **1989**, *1*, 476.

(30) (a) Wu, Y.-D.; Peng, Z.-H.; Xue, Z. *J. Am. Chem. Soc.* **1996**, *118*, 9772. (b) Wu, Y.-D.; Chan, K. W. K.; Xue, Z. *J. Am. Chem. Soc.* **1995**, *117*, 9259.

(31) Frisch, M. J.; Trucks, G. W.; Schlegel, H. B.; Gill, P. M. W.; Johnson, B. G.; Robb, M. A.; Cheeseman, J. R.; Keith, T.; Petersson, G. A.; Montgomery, J. A.; Raghavachari, K.; Al-Laham, M. A.; Zakrzewski, V. G.; Ortiz, J. V.; Foresman, J. B.; Peng, C. Y.; Ayala, P. Y.; Chen, W.; Wong, M. W.; Andres, J. L.; Replogle, E. S.; Gomperts, R.; Martin, R. L.; Fox, D. J.; Binkley, J. S.; Defrees, D. J.; Baker, J.; Stewart, J. P.; Head-Gordon, M.; Gonzalez, C.; Pople, J. A. *Gaussian 94*, revision B.3; Gaussian, Inc.: Pittsburgh, PA, 1995.

Scheme 2

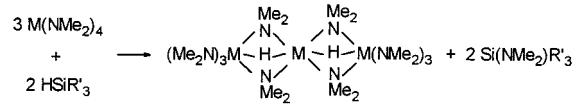

R'$_3$ = H$_2$Ph, HPh$_2$, HMePh, (NMe$_2$)Ph$_2$; M = Zr, **1**; Hf, **2**

solids showed no aminosilanes in the samples. Raman spectra of the solids showed M−N but no M−Si stretches. The black solids were extremely air-sensitive, pyrophoric, and readily hydrolyzed. The reaction of the black solids, which had been prepared with phenylsilanes, with 1 M DCl in D_2O yielded H_2, HD, and D_2 in ratios of 9:100:33 by MS, and $DNMe_2$, but no phenylsilanes as analyzed by GC/MS. These results indicated that the black solids prepared from the reactions of Ti(NMe$_2$)$_4$ with excess SiH_4 or phenylsilanes contained $-NMe_2$ and $-H$ ligands. The formation of a small amount of H_2 is perhaps the result of reductive elimination between hydride ligands in the black solids. The reduction of D^+ by the black solids probably yielded D_2. The heating of the reaction mixtures containing black solids and HSi(NMe$_2$)$_3$ gave powders **7** and **8** with compositions consistent with TiN and Si_3N_4, which is discussed below.

Reactions of M(NMe$_2$)$_4$ (M = Zr, Hf) with less than 1 equiv of $H_2SiR'Ph$ or HSi(NMe$_2$)Ph$_2$ were found to yield amide hydride complexes [(Me$_2$N)$_3$M(μ-H)(μ-NMe$_2$)$_2$]$_2$M (M = Zr, **1**; Hf, **2**), respectively (Scheme 2). The reactions of Zr(NMe$_2$)$_4$ were very fast, while the reactions of Hf(NMe$_2$)$_4$ were slightly slower. After dropwise addition of the silane to M(NMe$_2$)$_4$ (M = Zr, Hf) in Et_2O at room temperature was complete [and after an additional 10 min of stirring in the reactions of Hf(NMe$_2$)$_4$], the reaction mixture was cooled to −35 to −40 °C to yield solids of **1** and **2**. The solid was washed with cold Et_2O at −35 to −40 °C to remove the unreacted M(NMe$_2$)$_4$ and aminosilane HSi(NMe$_2$)Ph$_2$, and then recrystalized from Et_2O to give yellow crystals of **1** and colorless crystals of **2**. The reactions of M(NMe$_2$)$_4$ with less than 1 equiv of D_2SiPh_2 were found to give [(Me$_2$N)$_3$M(μ-D)(μ-NMe$_2$)$_2$]$_2$M (M = Zr, **1-*d*$_2$**; Hf, **2-*d*$_2$**), indicating that the hydrides in **1** and **2** were from the silane. **1** and **2** could be viewed as trinuclear complexes of yet unobserved HM(NMe$_2$)$_3$ (**3a**) or H_2M(NMe$_2$)$_2$ (**4a**) and unreacted M(NMe$_2$)$_4$.

The reactions between transition-metal complexes and silanes to give amide hydrides **1** and **2** are rare examples of such reactions. To our knowledge, the only other reported transition-metal amide reaction to give an isolated amide hydride complex involves a late transition-metal complex Cp*Ni(PEt$_3$)NHTol,[4] although main group (tin) amides have been reported to yield hydrides and aminosilanes in their reactions with silanes.[32] Buchwald and co-workers reported the formation of "Cp′$_2$Ti−H" [Cp′ = (*S*,*S*)-ethylenebis(η^5-tetrahydroindenyl)] or its equivalent in the reaction of Cp′$_2$TiF$_2$ with H_3SiPh and found it to be catalytically active for enantioselective imine hydrosilylation.[33] The proposed catalytic cycle involves reactions between "Cp′$_2$Ti−NR(*CHR$_1$R$_2$)" and H_3SiPh to give "Cp′$_2$Ti−H" and PhH$_2$Si−NR(*CHR$_1$R$_2$). The reactions of Cp$_2$MRR′ (M = Ti, Zr; R, R′ = H, alkyl, silyl)[34a−d] and Cp$_2$Ti(OPh)$_2$[34e] with silanes were found to give HR (HR′), disilanes, alkoxysilanes, and proposed M−H catalysts[34f] for polysilane synthesis. Such hydrides are believed to catalyze alkoxy- and siloxy-silane redistributions as well.[35] In the reactions of M−L multiple bonded complexes with silanes, silane additions to Ta=N bonds were reported, and Si intermediates containing Si−N bonds were proposed.[36] Clean reactions of silanes with Cp$_2$Zr=NBu^t were observed as well.[37] Silane additions to the Ti=S bond in Cp*$_2$Ti(=S)(Py),[38a,b] the Zr=O bond in Cp*$_2$Zr=O(Py),[38c] and the Ta=CHR bond in (RCH$_2$)$_3$Ta(PMe$_3$)=CHR (R = SiMe$_3$)[39] have also been reported.

The solids of amide hydride complexes [(Me$_2$N)$_3$M(μ-H)(μ-NMe$_2$)$_2$]$_2$M (M = Zr, **1**; Hf, **2**) are stable at room temperature, but decompose slowly in solution. **2** is also slightly light sensitive. **1** and **2** were found to react with H_2SiPh_2 and HSi(NMe$_2$)Ph$_2$ to give H_2, HSi(NMe$_2$)Ph$_2$, and Si(NMe$_2$)$_2$Ph$_2$, respectively, and unidentified species. Thus, in the preparation of **1** and **2**, once the dropwise addition of the silane was complete (and after 10 min of stirring in the preparation of **2**), the mixture solution was cooled to −35 to −40 °C to avoid further reactions of **1** and **2**.

The ^{1}H and ^{13}C{^{1}H} NMR spectra of [(Me$_2$N)$_3$M(μ-H)(μ-NMe$_2$)$_2$]$_2$M (M = Zr, **1**; Hf, **2**) are consistent with the structure assignment. The bridging hydrides in **1** were observed at 5.21 ppm in ^{1}H NMR at 23 °C. The resonance of bridging hydrides in the Hf analogue **2** was downfield shifted to 9.87 ppm in ^{1}H NMR at 23 °C. The amide resonances of **1** and **2** appear as one broad singlet at 2.98 (**1**) and 3.01 (**2**) ppm in ^{1}H NMR and 44.54 (**1**) and 44.25 (**2**) ppm in ^{13}C{^{1}H} NMR at 23 °C, indicating an exchange between the terminal and bridging amide ligands.

The variable-temperature ^{1}H NMR spectra of **1** were studied. Upon cooling a toluene-d_8 solution of **1**, the broad signal of amide ligands gradually disappeared to give separate bridging and terminal amide peaks. At −70 °C, there were one terminal and four distinct bridging amide resonances. At −50 °C, all bridging amide resonances first coalesced to give a single peak. The peaks of the bridging and terminal amide ligands coalesced at −20 °C. The first coalescence of the bridging amide resonances at −50 °C, followed by the coalescence of the bridging and terminal amide resonances, indicates that the rates of bridging/bridging ligand exchanges are faster than the bridging/terminal exchange. The estimated activation free energy of bridging/bridging ligand exchange $\Delta G^{\ddagger}_{222\ K}$ is 12.6 ± 0.5 kcal/mol. This bridging amide ligand exchange was perhaps the result of an internal rotation of the molecule with respect to the Zr−Zr−Zr axis.

Exchanges between bridging and terminal amide ligands are well-known.[40] Such an exchange was observed in, for example, (Me$_2$N)$_3$Zr(μ-Cl)$_2$(μ-NMe$_2$)Zr(NMe$_2$)$_2$(THF).[40] The activation

(32) Hays, D. S.; Fu, G. C. *J. Org. Chem.* **1997**, *62*, 7070.
(33) (a) Verdaguer, X.; Lange, U. E. W.; Reding, M. T.; Buchwald, S. L. *J. Am. Chem. Soc.* **1996**, *118*, 6784. (b) Verdaguer, X.; Lange, U. E. W.; Buchwald, S. L. *Angew. Chem., Int. Ed.* **1998**, *37*, 1103.
(34) (a) Gauvin, F.; Harrod, J. F.; Woo, H. G. *Adv. Organomet. Chem.* **1998**, *42*, 363. (b) Tilley, T. D. *Acc. Chem. Res.* **1993**, *26*, 22. (c) Corey, J. Y. In *Advances in Silicon Chemistry*; Larson, G. L., Ed.; JAI Press: Greenwich CT, 1991; Vol. 1, p 327. (d) Casty, G. L.; Lugmair, C. G.; Radu, N. S.; Tilley, T. D.; Walzer, J. F.; Zargarian, D. *Organometallics* **1997**, *16*, 8. (e) Bourg, S.; Corriu, R. J. P.; Enders, M.; Moreau, J. J. E. *Organometallics* **1995**, *14*, 564. (f) In the reactions of Cp$_2$MMe$_2$ with silanes, hydrides were isolated and characterized. See, e.g., Mu, Y.; Aitken, C.; Cote, B.; Harrod, J. F.; Samuel, E. *Can. J. Chem.* **1991**, *69*, 264.
(35) (a) Xin, S.; Aitken, C.; Harrod, J. F.; Mu, Y.; Samuel, E. *Can. J. Chem.* **1990**, *68*, 471. (b) Woo, H. G., Ph.D. Thesis, The University of California, San Diego, 1990.
(36) Gountchev, T. I.; Tilley, T. D. *J. Am. Chem. Soc.* **1997**, *119*, 12831.
(37) Lee, S.-Y.; Bergman, R. G. Unpublished results.
(38) (a) Sweeney, Z. K.; Polse, J. L.; Andersen, R. A.; Bergman, R. G.; Kubinec, M. G. *J. Am. Chem. Soc.* **1997**, *119*, 4543. (b) Sweeney, Z. K.; Polse, J. L.; Bergman, R. G.; Andersen, R. A. *Organometallics* **1999**, *18*, 5502. (c) Howard, W. A.; Trnka, T. M.; Waters, M.; Parkin, G. *J. Organomet. Chem.* **1997**, *528*, 95.
(39) (a) Diminnie, J. B.; Xue, Z. *J. Am. Chem. Soc.* **1997**, *119*, 12657. (b) Diminnie, J. B.; Blanton, J. R.; Cai, H.; Quisenberry, K. T.; Xue, Z. *Organometallics* **2001**, *20*, 1504.
(40) See, for example: Wu, Z.; Diminnie, J. B.; Xue, Z. *Inorg. Chem.* **1998**, *37*, 2570.

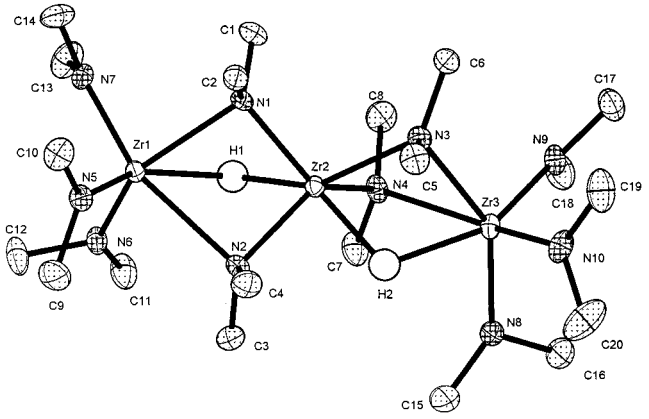

Figure 1. ORTEP diagram of **1**, showing 30% thermal ellipsoids.[41]

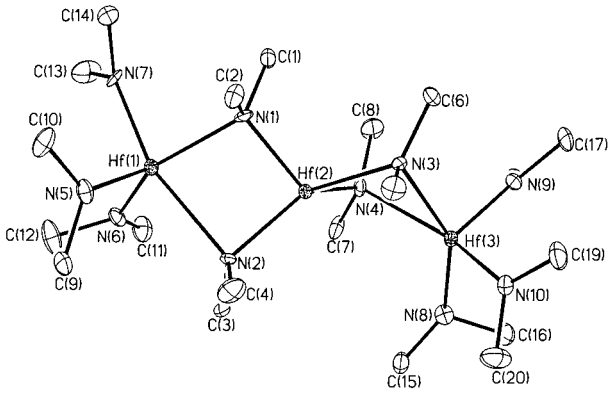

Figure 2. ORTEP diagram of **2**, showing 30% thermal ellipsoids.

free energy $\Delta G^{\ddagger}$ of 11.4 ± 0.5 kcal/mol for this exchange is comparable to that in **1**.

Crystal and Molecular Structures of 1 and 2. The crystal structures of amide hydride complexes $[(Me_2N)_3M(\mu\text{-}H)(\mu\text{-}NMe_2)_2]_2M$ (M = Zr, **1**; Hf, **2**) were determined by X-ray crystallography. ORTEPs of **1** and **2** are shown in Figures 1[41] and 2, respectively. The hydride ligands in **1** were located in an electron density map and independently refined. The crystal data and selected bond distances and bond angles are given in Tables 1 and 2 for **1** and Tables 1 and 3 for **2**. The structures of **1** and **2** consist of two terminal $M(NMe_2)_3$ moieties, one central M atom bridged to each terminal $M(NMe_2)_3$ by one hydride and two amide ligands.

To our knowledge, **1** and **2** are among the few structurally characterized Cp-free group 4 hydrides.[42,43] Others include neutron diffraction structure of $[P_2N_2]Zr(\mu\text{-}\eta^2\text{-}N_2H)(\mu\text{-}H)Zr[P_2N_2]$ $[P_2N_2 = PhP(CH_2SiMe_2NSiMe_2CH_2)_2PPh)]$,[43a] [H−Ti-

Table 1. Crystal Data for **1** and **2**

complex	**1**	**2**
formula	$C_{20}H_{62}N_{10}Zr_3$	$C_{20}H_{62}N_{10}Hf_3$
FW	716.46	978.27
crystal system	monoclinic	monoclinic
crystal color	yellow	colorless (plate)
space group	$P2_1/c$	$P2_1/c$
lattice parameters		
a (Å)	15.475(3)	14.5901(4)
b (Å)	8.613(2)	14.8647(5)
c (Å)	26.154(4)	17.0738(3)
β (deg)	106.310(10)	113.5665(13)
V (Å^3)	3345.7(11)	3394.05(19)
Z	4	4
d_{calcd} (Mg m^{-3})	1.422	1.914
μ (mm^{-1})	0.941	9.176
F(000)	1488	1872
temp (K)	173	173
2θ (deg)	3.24−45.1	3.04−56.42
no. of data collected	4589	19538
no. of independent data	4397 (R_{int} = 0.0382)	7792 (R_{int} = 0.0637)
refinement method	full-matrix least-squares on F^2	
R indices [$I > 2\sigma(I)$]	0.0314	0.0639
weighted R^a	0.0801 (wR^2)	0.1524 (wR^2)
goodness-of-fit on F^2 [a]	1.117	1.281

[a] $wR^2 = [\sum w(F_o^2 - F_c^2)^2/\sum w(F_o^2)^2]^{1/2}$; $R = \sum ||F_o| - |F_c||/\sum |F_o|$; $w = 1/[\sigma^2(F_o^2) + (aP)^2 + bP]$; $P = [2F_c^2 + \mathrm{Max}(F_o^2,0)]/3$

$(NN_2)]_2$ $[NN_2 = (Me_3SiNCH_2CH_2)_2NSiMe_3]$,[43b] a tripodal amide hydride Zr complex,[43c] $(2,6\text{-}Pr^i_2C_6H_3O)_3TiH(PMe_3)$,[43d] an adduct of NaH to a Zr porphyrinogen $[(\eta^5\text{-}\eta^1\text{-}\eta^1\text{-}\eta^1\text{-}Et_8N_4)Zr]_2(\mu\text{-}NaH)_2$,[43e] and BH_4^- complexes.[44] Some other known Cp-free group 4 hydrides include MH_2 (M = Ti, Zr, Hf),[45] silica-supported $(\equiv SiO)_3Zr-H$,[46a] and $HTi[(Me_3SiNCH_2CH_2)_3N]$.[46b] The average Zr−Zr distance of 3.232 Å in **1** reflects the constraints imposed by the bridging ligands.[44a−b] It is interesting to note that, in the structure of the only other known trinuclear Zr complex $Zr_3H_6(BH_4)_6(PMe_3)_4$,[44b] the Zr atoms are arranged in a nonlinear fashion with the Zr−Zr−Zr angle of 124.14(1)°. In contrast, the Zr atoms in **1** are almost linear with the Zr−Zr−Zr angle of 170.480(18)°. The middle and two terminal Zr atoms in **1** adopt a trigonal prismatic and trigonal antiprismatic geometries, respectively. The hydride ligands are closer to the central [av Zr(2)−H = 1.91(4) Å] than to the terminal Zr atoms [av Zr−H = 2.16(4) Å]. The Zr−H and Zr−N lengths are similar to those in other bridging Zr hydrides,[34f,43a,44a−d,47] and Zr amide complexes,[40] respectively. The Zr−N bonds between the bridging amides and central Zr(2) atom [$Zr-N_{av}$ = 2.174(4) Å] are longer than the bonds between terminal amide ligands and terminal Zr(1) and Zr(3) atoms [$Zr-N_{av}$ = 2.062(4) Å], but significantly shorter than the bonds between the bridging amides and the terminal Zr(1) and Zr(3) atoms [$Zr-N_{av}$ = 2.473(4) Å].

The Hf amide hydride complex **2** is similar to its Zr analogue **1**. The data set for **2** was not good enough to reveal the two bridging hydride ligands.[41] The three Hf atoms in **2** are nearly linear with an angle of 169.717(19) Å. The Hf−N bonds

(41) This ORTEP view of **1**, which is similar to that of **2** (Figure 2), is given so that the structure of the Zr complex **1** is better compared with that of its Hf analogue **2** where the hydrides were not located in the X-ray diffraction structure. A different ORTEP view of **1** has been published.[21]

(42) For group 4 metallocene and heterometallic hydrides, see: (a) Hlatky, G. G.; Crabtree, R. H. *Coord. Chem. Rev.* **1985**, *65*, 1. (b) Toogood, G. E.; Wallbridge, M. G. H. *Adv. Inorg. Chem. Radiochem.* **1982**, *25*, 267. (c) Wolczanski, P. T.; Bercaw, J. E. *Acc. Chem. Res.* **1980**, *13*, 121. (d) Labinger, J. A. In *Transition Metal Hydrides*; Dedieu, A., Ed.; VCH: New York, 1992; p. 361. (e) Etkin, N.; Hoskin, A. J.; Stephan, D. W. *J. Am. Chem. Soc.* **1997**, *119*, 11420. (f) Hart, D. W.; Schwartz, J. *J. Am. Chem. Soc.* **1974**, *96*, 8115.

(43) (a) Basch, H.; Musaev, D. G.; Morokuma, K.; Fryzuk, M. D.; Love, J. B.; Seidel, W. W.; Albinati, A.; Koetzle, T. F.; Klooster, W. T.; Mason, S. A.; Eckert, J. *J. Am. Chem. Soc.* **1999**, *121*, 523. (b) Love, J. B.; Clark, H. C. S.; Cloke, F. G. N.; Green, J. C.; Hitchcock, P. B. *J. Am. Chem. Soc.* **1999**, *121*, 6843. (c) Jia, L.; Ding, E.; Rheingold, A. L.; Rhatigan, B. *Organometallics* **2000**, *19*, 963. (d) Nöth, H.; Schmidt, M. *Organometallics* **1995**, *14*, 4601. (e) Jacoby, D.; Floriani, C.; Chiesi-Villa, A.; Rizzoli, C. *J. Am. Chem. Soc.* **1993**, *115*, 3595.

(44) (a) Gozum, J. E.; Girolami, G. S. *J. Am. Chem. Soc.* **1991**, *113*, 3829. (b) Gozum, J. E.; Wilson, S. R.; Girolami, G. S. *J. Am. Chem. Soc.* **1992**, *114*, 9483. (c) Mayo, S. C.; Bown, M.; Lloyd, V. K. *Acta Crystallogr.* **1994**, *C50*, 367. (d) Fryzuk, M. D.; Rettig, S. J.; Westerhaus, A.; Williams, H. D. *Inorg. Chem.* **1985**, *24*, 4316. (e) The structure of $ZrH_2(BH_4)_2(dmpe)_2$ has been determined by Baker, R. T.; Tebbe, F. N.; Calabrese, J. C. of DuPont.[44a]

(45) (a) Oka, A. *Bull. Chem. Soc. Jpn.* **1967**, *40*, 2284. (b) *The Merck Index*, 12th ed; Merck: Whitehouse Station, NJ, 1996. (c) TiH_4 in Kr and Ar matrixes at 12 K has been characterized by IR. Xiao, Z. L.; Hauge, R. H.; Margrave, J. L. *J. Phys. Chem.* **1991**, *95*, 2696. (d) $(dmpe)TiH_3$ has been reported. Tebbe, F. N. U.S. Patent No. 3933876, 1976.

(46) (a) Corker, J.; Lefebvre, F.; Lécuyer, C.; Dufaud, V.; Quignard, F.; Choplin, A.; Evans, J.; Basset, J.-M. *Science* **1996**, *271*, 966. (b) Cummins, C. C.; Schrock, R. R.; Davis, W. M. *Organometallics* **1992**, *11*, 1452.

(47) Jones, S. B.; Petersen, J. L. *Inorg. Chem.* **1981**, *20*, 2889.

Table 2. Selected Interatomic Distances and Angles in **1**

Zr(2)−H(2)	1.93(4)	Zr(2)−H(1)	1.88(4)	Zr(1)−N(7)	2.073(4)	Zr(2)−N(1)	2.231(4)
Zr(1)−H(1)	2.15(4)	Zr(3)−H(2)	2.16(4)	Zr(2)−N(2)	2.122(4)	Zr(2)−N(3)	2.215(4)
Zr(2)−Zr(1)	3.2296(8)	Zr(2)−Zr(3)	3.2348(7)	Zr(2)−N(4)	2.129(4)	Zr(3)−N(3)	2.393(4)
Zr(1)−N(1)	2.383(4)	Zr(1)−N(2)	2.556(4)	Zr(3)−N(4)	2.560(4)	Zr(3)−N(8)	2.049(4)
Zr(1)−N(5)	2.068(4)	Zr(1)−N(6)	2.041(4)	Zr(3)−N(9)	2.075(4)	Zr(3)−N(10)	2.066(4)
N(6)−Zr(1)−N(5)	107.48(16)	N(6)−Zr(1)−N(7)	97.10(17)	N(3)−Zr(2)−H(2)	72.7(11)	N(1)−Zr(2)−H(2)	149.4(12)
N(5)−Zr(1)−N(7)	102.94(16)	N(6)−Zr(1)−N(1)	144.17(15)	Zr(1)−Zr(2)−H(2)	134.3(11)	Zr(3)−Zr(2)−H(2)	40.4(11)
N(5)−Zr(1)−N(1)	104.39(15)	N(7)−Zr(1)−N(1)	91.28(14)	N(2)−Zr(2)−H(1)	78.2(13)	N(4)−Zr(2)−H(1)	82.7(13)
N(6)−Zr(1)−N(2)	92.37(15)	N(5)−Zr(1)−N(2)	87.52(13)	N(3)−Zr(2)−H(1)	147.4(12)	N(1)−Zr(2)−H(1)	70.9(13)
N(7)−Zr(1)−N(2)	162.99(14)	N(1)−Zr(1)−N(2)	72.96(12)	Zr(1)−Zr(2)−H(1)	39.7(13)	Zr(3)−Zr(2)−H(1)	134.5(13)
N(6)−Zr(1)−Zr(2)	104.73(11)	N(5)−Zr(1)−Zr(2)	119.26(11)	H(2)−Zr(2)−H(1)	132.9(17)	N(8)−Zr(3)−N(10)	96.20(16)
N(7)−Zr(1)−Zr(2)	122.38(11)	N(1)−Zr(1)−Zr(2)	43.68(9)	N(8)−Zr(3)−N(9)	109.24(16)	N(10)−Zr(3)−N(9)	103.84(15)
N(2)−Zr(1)−Zr(2)	41.00(8)	N(6)−Zr(1)−H(1)	80.3(11)	N(8)−Zr(3)−N(3)	144.04(14)	N(10)−Zr(3)−N(3)	91.42(14)
N(5)−Zr(1)−H(1)	151.5(12)	N(7)−Zr(1)−H(1)	103.2(11)	N(9)−Zr(3)−N(3)	102.85(14)	N(8)−Zr(3)−N(4)	91.74(14)
N(1)−Zr(1)−H(1)	63.8(11)	N(2)−Zr(1)−H(1)	64.5(11)	N(10)−Zr(3)−N(4)	162.59(14)	N(9)−Zr(3)−N(4)	87.99(14)
Zr(2)−Zr(1)−H(1)	34.0(12)	N(2)−Zr(2)−N(4)	129.29(14)	N(3)−Zr(3)−N(4)	73.30(12)	N(8)−Zr(3)−Zr(2)	105.13(10)
N(2)−Zr(2)−N(3)	131.07(15)	N(4)−Zr(2)−N(3)	85.87(14)	N(10)−Zr(3)−Zr(2)	121.59(11)	N(9)−Zr(3)−Zr(2)	118.25(11)
N(2)−Zr(2)−N(1)	84.91(13)	N(4)−Zr(2)−N(1)	131.42(14)	N(3)−Zr(3)−Zr(2)	43.20(9)	N(4)−Zr(3)−Zr(2)	41.07(8)
N(3)−Zr(2)−N(1)	94.93(13)	N(2)−Zr(2)−Zr(1)	52.21(10)	N(8)−Zr(3)−H(2)	78.6(10)	N(10)−Zr(3)−H(2)	102.4(10)
N(4)−Zr(2)−Zr(1)	122.29(10)	N(3)−Zr(2)−Zr(1)	141.80(9)	N(9)−Zr(3)−H(2)	151.5(10)	N(3)−Zr(3)−H(2)	65.4(10)
N(1)−Zr(2)−Zr(1)	47.52(9)	N(2)−Zr(2)−Zr(3)	123.36(10)	N(4)−Zr(3)−H(2)	64.0(10)	Zr(2)−Zr(3)−H(2)	35.4(10)
N(4)−Zr(2)−Zr(3)	52.18(10)	N(3)−Zr(2)−Zr(3)	47.71(9)	Zr(2)−N(3)−Zr(3)	89.09(13)	Zr(2)−N(1)−Zr(1)	88.80(12)
N(1)−Zr(2)−Zr(3)	141.85(10)	Zr(1)−Zr(2)−Zr(3)	170.480(18)	Zr(2)−N(4)−Zr(3)	86.75(13)	Zr(2)−N(2)−Zr(1)	86.79(12)
N(2)−Zr(2)−H(2)	83.0(11)	N(4)−Zr(2)−H(2)	76.7(12)				

Table 3. Selected Interatomic Distances and Angles in **2**

Hf(1)−N(5)	2.073(10)	Hf(1)−N(6)	2.081(10)	Hf(2)−N(3)	2.215(9)	Hf(2)−N(1)	2.215(10)
Hf(1)−N(7)	2.094(9)	Hf(1)−N(1)	2.383(10)	Hf(2)−Hf(3)	3.2085(6)	Hf(3)−N(8)	2.062(11)
Hf(1)−N(2)	2.514(9)	Hf(1)−Hf(2)	3.2173(6)	Hf(3)−N(9)	2.069(10)	Hf(3)−N(10)	2.071(11)
Hf(2)−N(4)	2.151(9)	Hf(2)−N(2)	2.160(9)	Hf(3)−N(3)	2.400(9)	Hf(3)−N(4)	2.571(10)
N(5)−Hf(1)−N(6)	105.1(4)	N(5)−Hf(1)−N(7)	101.0(4)	N(2)−Hf(2)−Hf(1)	51.3(2)	N(3)−Hf(2)−Hf(1)	140.9(2)
N(6)−Hf(1)−N(7)	97.1(4)	N(5)−Hf(1)−N(1)	101.3(4)	N(1)−Hf(2)−Hf(1)	47.8(3)	Hf(3)−Hf(2)−Hf(1)	169.717(19)
N(6)−Hf(1)−N(1)	149.9(4)	N(7)−Hf(1)−N(1)	91.5(4)	N(8)−Hf(3)−N(9)	104.4(4)	N(8)−Hf(3)−N(10)	95.9(4)
N(5)−Hf(1)−N(2)	90.1(4)	N(6)−Hf(1)−N(2)	92.2(4)	N(9)−Hf(3)−N(10)	106.1(4)	N(8)−Hf(3)−N(3)	149.4(4)
N(7)−Hf(1)−N(2)	163.1(4)	N(1)−Hf(1)−N(2)	73.7(3)	N(9)−Hf(3)−N(3)	102.3(4)	N(10)−Hf(3)−N(3)	90.9(4)
N(5)−Hf(1)−Hf(2)	120.1(3)	N(6)−Hf(1)−Hf(2)	109.1(3)	N(8)−Hf(3)−N(4)	91.9(4)	N(9)−Hf(3)−N(4)	90.6(4)
N(7)−Hf(1)−Hf(2)	121.1(3)	N(1)−Hf(1)−Hf(2)	43.5(2)	N(10)−Hf(3)−N(4)	159.1(4)	N(3)−Hf(3)−N(4)	73.1(3)
N(2)−Hf(1)−Hf(2)	42.1(2)	N(4)−Hf(2)−N(2)	130.5(4)	N(8)−Hf(3)−Hf(2)	108.1(3)	N(9)−Hf(3)−Hf(2)	121.4(3)
N(4)−Hf(2)−N(3)	85.5(4)	N(2)−Hf(2)−N(3)	129.9(4)	N(10)−Hf(3)−Hf(2)	117.3(3)	N(3)−Hf(3)−Hf(2)	43.6(2)
N(4)−Hf(2)−N(1)	132.6(4)	N(2)−Hf(2)−N(1)	84.4(4)	N(4)−Hf(3)−Hf(2)	41.9(2)	Hf(2)−N(1)−Hf(1)	88.7(3)
N(3)−Hf(2)−N(1)	94.1(3)	N(4)−Hf(2)−Hf(3)	53.0(3)	f(2)−N(2)−Hf(1)	86.6(3)	Hf(2)−N(3)−Hf(3)	88.0(3)
N(2)−Hf(2)−Hf(3)	121.0(2)	N(3)−Hf(2)−Hf(3)	48.4(2)	Hf(2)−N(4)−Hf(3)	85.1(3)		
N(1)−Hf(2)−Hf(3)	142.2(3)	N(4)−Hf(2)−Hf(1)	124.7(3)				

between the bridging amides and central Hf(2) atom [Hf−N_{av} = 2.185(10) Å] are longer than the bonds between terminal amide ligands and terminal Hf(1) and Hf(3) atoms [Hf−N_{av} = 2.075(11) Å], but significantly shorter than the bonds between the bridging amides and the terminal Hf(1) and Hf(3) atoms [Hf−N_{av} = 2.467(10) Å]. The average terminal Hf−N length of 2.075(11) Å in **2** is close to that [2.084(3) Å] in [(ArylNCH$_2$-CH$_2$)$_2$O]HfEt$_2$ (Aryl = 2,6-Pr$^i_2$C$_6$H$_3$).[48] Although the structures of these two Zr and Hf amide hydride complexes are similar, the crystals of **1** and **2** are not isomorphous.[22]

Reversible Reactions of $(Me_2N)_3ZrSi(SiMe_3)_3$ (5) with Silanes To Yield Zr Hydride (6) and Aminosilanes. The reactions of Zr−amide bonds with silanes were further studied with $(Me_2N)_3ZrSi(SiMe_3)_3$ (**5**),[25] where the Zr−silyl bond may compete with the Zr−amide bonds in the reactions. The reactions of **5** with $H_2SiR'Ph$ (R′ = H, Ph, Me) were found to give an unstable hydride complex $(Me_2N)_2Zr(H)Si(SiMe_3)_3$ (**6**) and aminosilanes $HSi(NMe_2)R'Ph$, and there was no sign of reactions of the Zr−$Si(SiMe_3)_3$ bond with the silanes. To our surprise, the reactions to give **6** were reversible and reached equilibria (Scheme 3-I). The equilibrium **5** + H_2SiPh_2 ⇄ **6** + $HSi(NMe_2)Ph_2$ was found to favor **5** and H_2SiPh_2 at 0 °C, as shown in the equilibrium constant K_{eq} [0.11(0.01)] and $\Delta G°$ [1.20(0.05) kcal/mol] at this temperature. In a separate equilibrium (Scheme 3-I) involving $H_2SiMePh$ [**5** + $H_2SiMePh$ ⇄ **6** + $HSi(NMe_2)MePh$], the addition of $HSi(NMe_2)Ph_2$ to a solution in equilibrium yielded H_2SiPh_2. This observation confirmed that the reactions of these d^0 amide complexes with silanes to form hydrides and aminosilanes were reversible. To our knowledge, the current study represents the first direct observation of hydrides in the reactions of transition-metal amides with silanes through unusual equilibria.[4] The decomposition of **5** gave $HSi(SiMe_3)_3$ and other unknown species.

Scheme 3. Exchanges between **5** and **6** (I) and between **6**-d_1 and $H_2SiR'Ph$ (R′ = H, Me) (II)

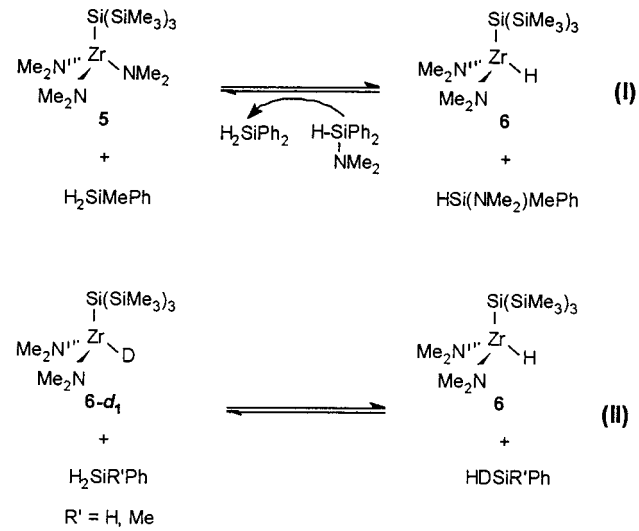

$(Me_2N)_2Zr(D)Si(SiMe_3)_3$ (**6**-d_1), prepared from the reaction

(48) Aizenberg, M.; Turculet, L.; Davis, W. M.; Schattenmann, F.; Schrock, R. R. *Organometallics* **1998**, *17*, 4795.

of **5** with $D_2SiMePh$, was found to undergo hydrogen exchange with $H_2SiMePh$ in benzene-d_6 to give HDSiMePh and $(Me_2N)_2Zr(H)Si(SiMe_3)_3$ (**6**) (Scheme 3-II). HDSiMePh was characterized by a 1:1:1 triplet of *H*-Si at 4.423 ppm and its isotopic shift (0.009 ppm) from the resonance of *H*-Si in $H_2SiMePh$. Subsequent H−D exchanges between $(Me_2N)_2Zr(H)Si(SiMe_3)_3$ (**6**) and $DSi(NMe_2)MePh$, which was yielded in the initial step, led to the formation of $HSi(NMe_2)MePh$ observed in NMR. ^1H NMR of the solution thus showed presence of **6-*d*$_1$**, **6**, $D_2SiMePh$, HDSiMePh, $H_2SiMePh$, $DSi(NMe_2)MePh$, and $HSi(NMe_2)MePh$. A similar H−D exchange was observed between H_3SiPh and **6-*d*$_1$**, which was prepared from **5** and D_3SiPh. No exchange between $D_2SiMePh$ and $H_2SiMePh$ was observed in the absence of the metal complex $(Me_2N)_2Zr(H)Si(SiMe_3)_3$ (**6**) in a control experiment. Such exchanges perhaps proceed through σ-bond metathesis involving M−H and D−Si bonds. Similar exchanges involving lanthanide hydrides $[(Bu^tCp)_2Ln(\mu\text{-}H)]_2$ and surface-bound $(\equiv Si-O)_3Zr-H$ and deuteriosilanes were recently reported.[49]

Preparation and Characterization of Ti−Si−N Ternary Powders and Thin Films from the Reaction of $Ti(NMe_2)_4$ with SiH_4. The studies of the reaction of $Ti(NMe_2)_4$ and SiH_4 to give solid materials were conducted both at 23 °C, followed by heating, in a Schlenk system and at high temperatures (ca. 450 °C) in an ultrahigh vacuum chemical vapor deposition (CVD) reactor.[22,29] The former gave powders **7** and **8** (which were used to better understand the reaction) and the black solid as a reaction product. The latter led to the deposition of the Ti−Si−N thin film **9**.

In the preparation of powders **7** and **8**, liquid $Ti(NMe_2)_4$ at room temperature was first exposed to excess SiH_4 to give a mixture of a black solid and $HSi(NMe_2)_3$, which was discussed earlier. The mixture was then heated at 700−1090 °C to give amorphous powders with a metallic appearance under a microscope.

We designed our CVD system to only allow the two precursors to mix exactly above the substrate in the heating zone to avoid premature reaction between the silane and $Ti(NMe_2)_4$, a volatile liquid at room temperature with a boiling point of 60 °C at 0.1 Torr. One feature of our process was that the deposition was direction-oriented. When the substrate was placed parallel to the gas flow, no deposition occurred. We thus placed the substrate with one end slightly tilted in the direction of the gas flow to give the observed thin film deposition. In addition, the minimum delivery zone temperature in our system was found to be 250 °C if the deposition temperature was set to 450 °C.

Several techniques including X-ray photoelectron spectroscopy (XPS),[28] Rutherford backscattering spectrometry (RBS),[28] and energy dispersive spectroscopy (EDS) were used to analyze the film and powders in the current studies.[28,50] The XPS chemical shifts of Ti 2$p_{3/2}$, Si 2*p*, N 1*s*, and O 1*s* in the film **9**, powder **8**, and other known solids related to Ti−Si−N ternary alloys are given in Table 4. The Ti:Si:N ratios in the film were obtained from RBS.

XRD of powder **7** showed the diffraction pattern of TiN. When the heating of the mixture from the reaction between $Ti(NMe_2)_4$ and SiH_4 was conducted at 1000 °C, XRD showed the powder was amorphous. The XPS of powder **8** revealed that the binding energy of the Ti 2$p_{3/2}$ peak (454.90 eV) in powder **8** was nearly the same as that in TiN (454.8 eV).[50a] In comparison, the binding energies of Ti 2$p_{3/2}$ peak in TiO_2 and $TiSi_2$ are 458.7 and 453.6 eV, respectively.[50b] The N 1*s* peak (396.60 eV) in powder **8** is close to those observed for TiN (396.9 eV)[16a] and Si_3N_4(O) (397.5 eV) as well.[50a] The Si 2*p* peak (101.20 eV) in powder **8** is close to that in Si_3N_4(O) (101.7 eV), but significantly shifted from those in $TiSi_n$ and SiO_2 (Table 4).[50a] In addition, the binding energies of Ti 2$p_{3/2}$, N 1*s*, and Si 2*p* in powder **8** were close to those in the reported $TiSi_{1.4}N$ ternary alloy.[50c] These XPS analyses indicated that TiN and Si_3N_4(O) were likely present in powder **8**. EDS (energy dispersive spectroscopy) analyses gave Ti:Si ratio of 1.5:1 in powder **8**.

Table 4. XPS Chemical Shifts of Solid Compounds Related to Ti−Si−N Ternary Alloys and Samples in This Study

	binding energies (eV)			
solid compounds[a]	Ti 2$p_{3/2}$	Si 2*p*	N 1*s*	O 1*s*
TiN[16a]	454.8		396.9	
Si_3N_4(O)[50a]		101.7	397.5	531.3
Si_3N_4[50a]		104.5	400.50	
TiSi[50b] ($TiSi_2$[50b])	453.3 (453.6)	98.5 (99.0)		
$TiSi_{1.4}N$[50c]	455.5	102.5	397.8	
powder **8** (after sputtering)	454.90	101.20	396.60	531.40
film **9** (after sputtering)	455.50	102.00	397.00	531.00

[a] The binding energies of following impurities are: Ti 2$p_{3/2}$ at 458.3−459.0 eV and O 1*s* at 533.3 eV in TiO_2;[50d] Si 2*p* at 103.1 eV and O 1*s* at 532.4 eV in SiO_2.[50a]

The Rutherford backscattering spectra (RBS) of film **9** showed that the film was not oriented since the random and aligned spectra for Ti, Si (in film), and N were identical. The Ti:Si:N ratios in film **9** by RBS were 16:13:30. These ratios are close to those expected for TiN−Si_3N_4, and Ti:Si ratio of 1.2:1 in film **9** is close to that in powder **8**. The XPS binding energies of film **9** are listed in Table 4 along with data reported in the literature. The binding energies of Ti 2$p_{3/2}$, Si 2*p*, and N 1*s* peaks in film **9** after sputtering are close to those in the reported $TiSi_{1.4}N$ ternary alloy[50c] and in powder **8**. Another Si 2*p* peak was observed at 98.5 eV in film **9**, which corresponded to Si wafer substrate. There was also oxygen in the film which likely came from the oxidized layer of the silicon wafer or the reaction of the film with residual O_2 in the XPS chamber during data collection. Similar O incorporation has been reported in the deposition of TiN film from $Ti(NMe_2)_4$ and NH_3, especially when not enough NH_3 was supplied.[51] The carbon binding energies in XPS showed the carbon in film **9** was mainly hydrocarbons with some TiC.[52] Carbon contamination has been also observed in CVD of TiN from $Ti(NMe_2)_4$ and NH_3.[16a,20] Transamination with NH_3 to give $Ti-NH_2$ was used to reduce carbon contamination.[16,20] Recent studies suggested that β-H abstraction by a coordinated $-NR_2$ ligand contributed to the C incorporation in the TiN films.[16b]

The current studies focused on mechanistic pathways in the formation of Ti−N−Si ternary films from the reactions of $Ti(NR_2)_4$ with SiH_4. We thus did not attempt to improve the qualities of powders **7** and **8** and film **9**. The results here showed that the reaction between $Ti(NMe_2)_4$ and SiH_4, followed by heating, likely gave TiN−Si_3N_4 ternary powders and a film of mixtures of TiN−Si_3N_4 at a high temperature in a CVD reactor.

(49) (a) Voskoboynikov, A. Z.; Parshina, I. N.; Shestakova, A. K.; Butin, K. P.; Beletskaya, I. P.; Kuz′mina, L. G.; Howard, J. A. K. *Organometallics* **1997**, *16*, 4041. (b) Coutant, B.; Quignard, F.; Choplin, A. *J. Chem. Soc., Chem. Commun.* **1995**, 137.

(50) (a) Shalaeva, E. V.; Borisov, S. V.; Denisov, O. F.; Kuznetsov, M. V. *Thin Solid Films* **1999**, *339*, 129. (b) Nemoshkalenko, V. V.; Zakharov, A. I.; Aleshin, V. G.; Matveev, Yu. A. *Theor. Exp. Chem. (Engl. Transl.)* **1977**, *13*, 529. (c) Miura, Y.; Fujieda, S. *J. Appl. Phys.* **1997**, *81*, 6476. (d) Armstrong, N. R.; Quinn, R. K. *Surf. Sci.* **1977**, *67*, 451.

(51) Musher, J. N.; Gordon, R. G. *J. Electrochem. Soc.* **1996**, *143*, 736.

(52) C 1*s* peak for film **9** was observed at 284.5 eV in XPS. In comparison, C 1*s* at 281.6 eV in TiC and at 284.4 eV in hydrocarbons were reported (Girolami, G. S.; Jensen, J. A.; Pollina, D. M.; Williams, W. S.; Kaloyeros, A. E.; Allocca, C. M. *J. Am. Chem. Soc.* **1987**, *109*, 1579).

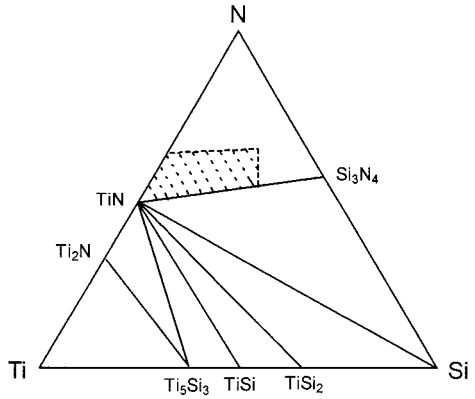

Figure 3. Schematic representation of phase equilibria in the Ti−Si−N system at 1000 °C.[53] The area with broken lines represents the compositions of $TiN-Si_3N_4$ ternary materials prepared from the reactions of $Ti(NEt_2)_4$ with SiH_4 and NH_3.[8]

In other words, the compositions of the powders and film prepared at room- and high temperatures suggested that similar chemistry and mechanistic pathways took place in a large temperature range. The ternary materials are likely $TiN-Si_3N_4$, and it is unlikely that $TiSi_n$ is present in the reaction products. The Ti, Si, and N composition in film **9** from RBS places it near the $TiN-Si_3N_4$ tie line in the Ti−Si−N phase diagram (Figure 3).[7c,8,53] Similar ternary films ($TiN-Si_3N_4$) have been reported by Nicolet, Smith, and co-workers in the CVD from the reaction of $Ti(NEt_2)_4$ with SiH_4 and NH_3.[7c,8] The compositions of Ti, N, and Si in these films placed them near or above the TiN and Si_3N_4 tie line as well in the Ti−Si−N phase diagram. The C impurity levels in the films by Smith and co-workers are low perhaps due in part to the use of $-NEt_2$ ligand rather than $-NMe_2$ ligand in $Ti(NR_2)_4$.[20]

Ab Initio MO Calculations on the Reactions of $Ti(NR_2)_4$ and $HTi(NH_2)_3$ (3b) with SiH_4, H_3Si-NH_2, and $H_2Si(NH_2)_2$. Theoretical calculations were carried out to study the reactions of model complexes $Ti(NR_2)_4$ (R = H and Me) with SiH_4 and the fate of the intermediates $HTi(NH_2)_3$ (**3b**) and H_3Si-NH_2.[54] Model $Ti(NH_2)_4$ was chosen for $Ti(NMe_2)_4$ for most of the calculations to reduce computing time. This analysis through the calculations holds true only if the simplified model represents well the actual molecule. In this case, this assumption is valid, since the geometries of both simplified model and actual molecule are close.

As indicated in Scheme 1, there are two possible pathways for the σ-bond metathesis reactions between $Ti(NR_2)_4$ and SiH_4. The two transition structures **A** and **B** lead to the formation of aminosilane H_3Si-NH_2 and ammonia NH_3, respectively. The two calculated transition structures **A** and **B** (HF/HW3) are given in Figure 4, and the calculated energetic parameters are shown in Table 5. All energies will be discussed based on the MP2/HW3 values. Transition structure **B** mainly involves the transfer of a hydrogen from Si to a $-NH_2$ ligand. The activation energy is calculated to be high (37.0 kcal/mol). The reaction is also highly endothermic with ΔH_{298} of 24.7 kcal/mol, reflecting the fact that a stronger Ti−N bond is replaced by a weaker Ti−Si bond. Transition structure **A** giving aminosilane H_3Si-NH_2 has lower activation energy than **B** by about 18.8 kcal/mol. This strongly supports the experimental observations that only metal hydride complexes were formed in the reactions $M(NMe_2)_4$ with SiH_4. The four-membered ring transition structure **A** is in distorted trigonal-bipyramidal geometry with the hydrogen delivering from the axial direction. The transition structure **C** in the reaction of $Ti(NMe_2)_4$ with SiH_4 was also calculated. The geometry of this transition structure and the activation energy of the reaction are very similar to **A**, suggesting that $Ti(NH_2)_4$ is a good model for $Ti(NMe_2)_4$ in the reaction with SiH_4.

The fate of the intermediate H_3Si-NH_2 was also investigated. It was assumed that H_3Si-NH_2 produced initially could react with $Ti(NH_2)_4$ to give $H_2Si(NH_2)_2$, which in turn, could further react with $Ti(NH_2)_4$ to give $HSi(NH_2)_3$. Transition structures **E** and **F** are for the reactions of $Ti(NH_2)_4$ with H_3Si-NH_2 and $H_2Si(NH_2)_2$, respectively. While structure **E** is very similar to **A**, structure **F** is much later, as indicated by a shorter Ti−H bond and a significantly elongated Si−H bond. Interestingly, both H_3Si-NH_2 and $H_2Si(NH_2)_2$ are predicted to be more reactive (activation enthalpy of 11.8 and 16.0 kcal/mol, respectively) than SiH_4 (18.2 kcal/mol). H_3Si-NH_2 appears to be particularly reactive. This is in agreement with the experimental results that only $H_2Si(NMe_2)_2$ and $HSi(NMe_2)_3$ were observed as reaction intermediates. All efforts in locating a transition structure for the reaction of $Ti(NH_2)_4$ with $HSi(NH_2)_3$ to give $HTi(NH_2)_3$ and $Si(NH_2)_4$ failed. Apparently, $HSi(NH_2)_3$ has lower reactivity because of its bulkiness.

Ab initio calculations also showed that reactions of the hydride intermediate $HTi(NH_2)_3$ (**3b**) with SiH_4 or H_3Si-NH_2 through σ-bond metathesis reactions to give $H_2Ti(NH_2)_2$ (**4b**) are favored. These two transition structures are given as **G** and **H** (Figure 5). Once again, these metathesis transition structures are quite similar to **A** and **E**. The calculated activation energy for the reaction of $HTi(NH_2)_3$ (**3b**) with SiH_4 is about 21.3 kcal/mol. This is slightly higher than that of $Ti(NH_2)_4$ with SiH_4 (Table 5). The reaction of $HTi(NH_2)_3$ (**3b**) with H_3Si-NH_2 to give $H_2Ti(NH_2)_2$ (**4b**) + $H_2Si(NH_2)_2$ has a lower activation energy of 14.4 kcal/mol. Once again, the H_3Si-NH_2 is more reactive. The calculated preferential formation of $HTi(NH_2)_3$ (**3b**) and $H_2Ti(NH_2)_2$ (**4b**) in the gas phase is consistent with the observations of hydride complexes **1** and **2** (Figures 1 and 2) in the solid state as trinuclear complexes of $HM(NMe_2)_3$ (**3a**) and $H_2M(NMe_2)_2$ (**4a**) and unreacted $M(NMe_2)_4$. The calculated preferential formation of **3b** and **4b** is also consistent with the observations of $-NMe_2$ and $-H$ ligands in the black solids from the reactions of $Ti(NMe_2)_4$ with SiH_4.

The reaction $HTi(NH_2)_3$ (**3b**) + $SiH_4 \rightarrow Ti(NH_2)_3(SiH_3)$ + H_2 through transition state **I** was also studied. In contrast to structure **A**, **I** has a considerable Ti−Si bond formation.[55] The two Ti−H distances in **I** are about the same. This and the calculated lower activation energy indicate that hydride in **3b** is a better leaving group than amido group in this case. The calculated activation energy is about 25.6 kcal/mol, which is higher than that (21.3 kcal/mol) to give $H_2Ti(NH_2)_2$ (**4b**) and H_3Si-NH_2 by about 4 kcal/mol indicating that this pathway is unlikely.

It should be noted that all these metathesis reactions are endothermic. For example, the reaction of $Ti(NH_2)_4$ with SiH_4 to give $H-Ti(NH_2)_3-H_2N-SiH_3$ complex (**D**) is endothermic by about 10 kcal/mol. So what is the driving force for the reactions? Calculations were carried out for the dimerization of $Ti(NH_2)_4$ and $H-Ti(NH_2)_3$ and complexation of $Ti(NH_2)_4$ with $HTi(NH_2)_3$ (**3b**). The calculated complexes are given as

(53) Beyers, R.; Sinclair, R.; Thomas, M. E. *J. Vac. Sci. Technol.* **1984**, *B2*, 781. The use of this phase diagram is, however, tentative, as it was obtained at 1000 °C. It is, to our knowledge, the best simplied Ti−Si−N phase diagram in the literature. For a more detailed Ti−Si−N phase diagram, see: Sambasivan, S.; Petuskey, W. T. *J. Mater. Res.* **1994**, *9*, 2362.

(54) H_3Si-NH_2 has been reported. Beach, D. B. *Inorg. Chem.* **1992**, *31*, 4174.

(55) Cundari and Gordon conducted ab initio quantum chemical analysis of the conversion $H_2(X)M-NH_2 \rightarrow H_2M{=}NH + HX$ (M = Ti, Zr, Hf; X = SiH_3, H, Me, Cl, NH_2). Cundari, T. R.; Gordon, M. S. *J. Am. Chem. Soc.* **1993**, *115*, 4210.

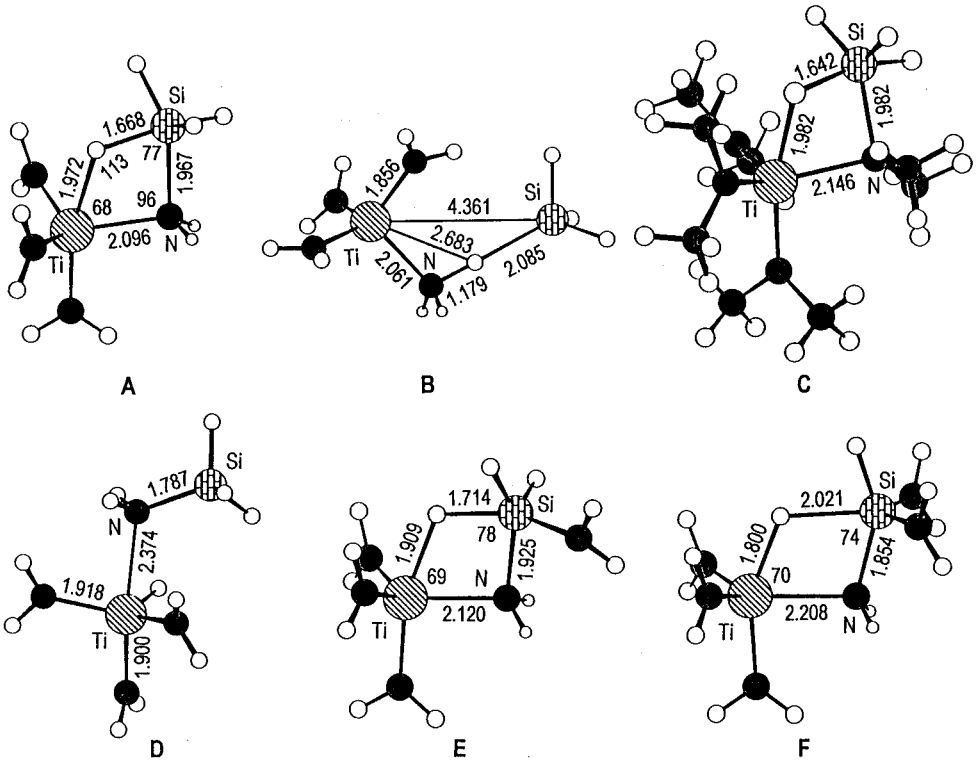

Figure 4. Calculated geometries (HF/HW3) of transition structures and product for the reactions of $Ti(NH_2)_4$ with SiH_4 (**A**, **B**, **D**), H_3Si-NH_2 (**E**), and $H_2Si(NH_2)_2$ (**F**), and of $Ti(NMe_2)_4$ with SiH_4 (**C**) (bond distances: Å; bond angles: deg).

Table 5. Calculated Changes in Entropies (ΔS_{298}, cal/mol·K) and Enthalpies (ΔH_{298}, kcal/mol) for the Formation of Transition Structures and Products of the Reactions of Titanium Amide Compounds with Silanes

		HF/3-21G*		HF/HW3	MP2/HW3
entry	reaction	ΔS_{298}	ΔH_{298}	ΔH_{298}	ΔH_{298}
1	$Ti(NH_2)_4 + SiH_4 \rightarrow$ **A**	−41.7	45.8	28.8	18.2
2	$Ti(NH_2)_4 + SiH_4 \rightarrow$ **4a** $+ NH_3$	11.0	65.5	27.3	24.7
3	$Ti(NH_2)_4 + SiH_4 \rightarrow$ **B**	−28.6	70.9	46.9	37.0
4	$Ti(NH_2)_4 + SiH_4 \rightarrow$ **D**	−38.3	31.3	12.3	10.0
5	$Ti(NMe_2)_4 + SiH_4 \rightarrow$ **C**	−47.4	54.7	38.2	19.5
6	$Ti(NH_2)_4 + H_3Si-NH_2 \rightarrow$ **E**	−52.9	39.1	22.9	11.8
7	$Ti(NH_2)_4 + H_2Si(NH_2)_2 \rightarrow$ **F**	−45.5	38.8	24.7	16.0
8	$HTi(NH_2)_3 + SiH_4 \rightarrow$ **G**	−40.2	48.3	30.3	21.3
9	$HTi(NH_2)_3 + H_3Si-NH_2 \rightarrow$ **H**	−50.2	38.6	23.4	14.4
10	$HTi(NH_2)_3 + SiH_4 \rightarrow$ **I**	−34.5	74.4	50.7	25.6
11	$Ti(NH_2)_4 + Ti(NH_2)_4 \rightarrow$ **J**	−58.3	−31.5	−15.5	−28.2
12	$Ti(NH_2)_4 + HTi(NH_2)_3 \rightarrow$ **K**	−45.0	−24.4	−13.4	−28.6
13	$HTi(NH_2)_3 + HTi(NH_2)_3 \rightarrow$ **L**	−38.2	−10.8	−4.4	−21.9

J−**L** in Figure 5. It appears that the complexation of $Ti(NH_2)_4$ with $HTi(NH_2)_3$ (**3b**) to give **K**, which has one hydrogen and one amido bridges, is most favorable of the three processes. This is in full agreement with experimental observations of trinuclear complexes $[(Me_2N)_3M(\mu\text{-}H)(\mu\text{-}NMe_2)_2]_2M$ (M = Zr, **1**; Hf, **2**) (Scheme 2 and Figures 1 and 2), which can be formed either by one $H_2M(NMe_2)_2$ (**4a**) with two $M(NMe)_4$ or by two $HM(NMe_2)_3$ (**3a**) with one $M(NMe_2)_4$. It is proposed that this complexation provides the driving force for the metathesis reactions.

Reactions of $M(NMe_2)_4$ (M = Ti, Zr, Hf) with Silanes: Mechanistic Considerations. Both the experimental and theoretical studies suggested that $M(NMe_2)_4$ (M = Ti, Zr, Hf) and silanes undergo σ-bond metathesis through transition state **A** (Scheme 1 and Figure 4). Nevertheless, if such reactions proceed through **B**, the amine HNR_2 (or NH_3) thus produced could further react with silanes to form aminosilanes and H_2 in the presence of a catalyst.[56] To exclude this pathway, we investigated whether $HNMe_2$ could survive the conditions of the reaction between $Zr(NMe_2)_4$ and H_2SiPh_2. Our studies suggest that the reaction of $HNMe_2$ with H_2SiPh_2, if it occurred, would be much slower than that of $Zr(NMe_2)_4$ with H_2SiPh_2. It is unlikely that $HNMe_2$ was produced through the transition state **B** in Scheme 1, and then reacted with H_2SiPh_2 to give the aminosilane. Although we cannot rule out transition state **B**, the isolation of amide hydride complexes **1** and **2**, the observation of $(Me_2N)_2Zr(H)Si(SiMe_3)_3$ (**6**), and the ab initio MO calculations indicate that transition state **A** is more likely and favored. We recently found that the reactions of the Ta=CHR ligand in a metal alkylidene complex $(Me_3SiCH_2)_3Ta(PMe_3)$-[=CHSiMe$_3$] with phenyl-containing silanes $H_2SiR'Ph$ (R′ = H, Me, Ph), followed similar pathways with the formation of a disilylalkylidene product.[39]

The studies presented here indicated that the first step in the CVD of Ti−Si−N thin films involving $Ti(NMe_2)_4$ and SiH_4 yielded $HTi(NMe_2)_3$ (**3a**) and $H_3Si(NMe_2)$ (Scheme 4). The analyses of the black solids suggested that in the following steps similar reactions occurred to give black solids containing hydride and unreacted amide ligands. The role of silane here was to remove amide ligands [as aminosilanes $H_nSi(NMe_2)_{4-n}$ (n = 1, 2)]. Subsequently, the two types of products, the black solids containing −H and $-NMe_2$, and the aminosilanes $H_nSi(NMe_2)_{4-n}$, perhaps underwent *separate* thermal decompositions to give TiN and Si_3N_4, respectively (Scheme 4). In other words, the reaction pathways led to the formation of the two types of intermediates (the black solids and aminosilanes) that likely yielded the two solid compounds observed in the Ti−Si−N ternary films. $H_nSi(NMe_2)_{4-n}$ have been used as precursors in chemical vapor deposition of Si_3N_4.[57] The reactivity of the Ti−NMe_2 and H−Si bonds seemed to forbid the formation of intermediates with Ti−Si bonds. This perhaps explained in part why silicides $TiSi_n$ were either not present or not the major products in the Ti−

(56) (a) Liu, H. Q.; Harrod, J. F. *Organometallics* **1992**, *11*, 822. (b) Laine, R. M.; Blum, Y. D.; Tse, D.; Glaser, R. *ACS Symp. Ser.* **1988**, *360*, 124. (c) Kinsley, K. K.; Nielson, T. J.; Barton, T. J. *Main Group Met. Chem.* **1987**, *10*, 307.

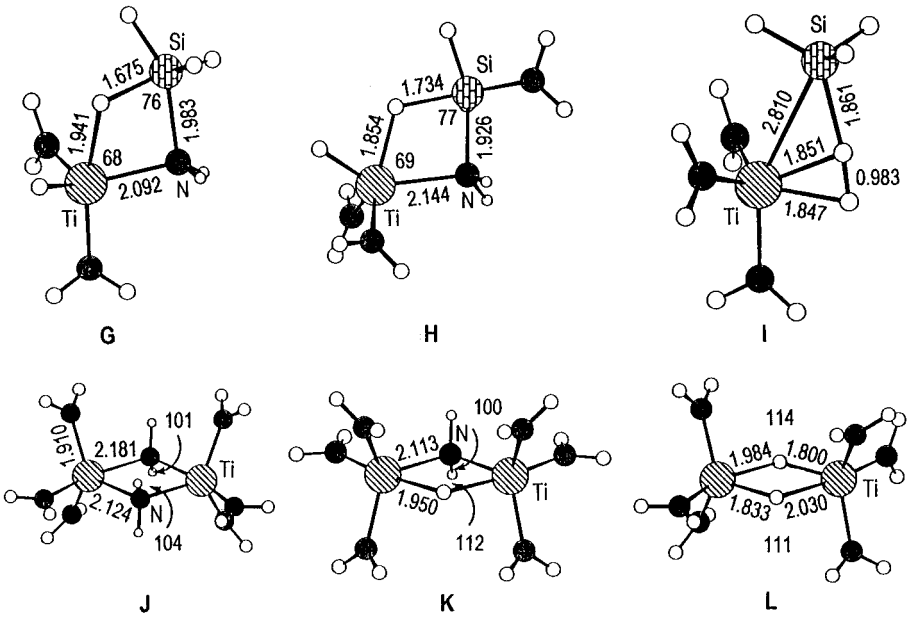

Figure 5. Calculated geometries (HF/HW3) of the transition structures for the reactions of HTi(NH$_2$)$_3$ (**3b**) with SiH$_4$ (**G** and **I**) and H$_3$Si−NH$_2$ (**H**) as well as calculated geometries (HF/HW3) of complexes [Ti(NH$_2$)$_4$]$_2$ (**J**) and [HTi(NH$_2$)$_3$]$_2$ (**L**), and an adduct of HTi(NH$_2$)$_3$ with Ti(NH$_2$)$_4$ (**K**) (bond distances: Å; bond angles: deg).

Scheme 4. Proposed Pathways in the Reaction of Ti(NMe$_2$)$_4$ with SiH$_4$ to Give TiN−Si$_3$N$_4$ as Ti−Si−N Ternary Materials

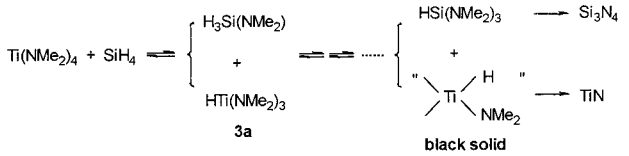

Si−N ternary films. Transamination aside, similar pathways may be present in the reactions of Ti(NEt$_2$)$_4$ with SiH$_4$ and NH$_3$ and deposition of TiN−Si$_3$N$_4$ ternary films from these reactions.[8] It is important to point out that SiH$_4$ and NH$_3$, either alone or mixtures thereof, are unreactive at low temperatures. To grow Si$_3$N$_4$ from SiH$_4$−NH$_3$ requires temperatures over 800 °C.[58] Thus, the intermediates such as HSi(NMe$_2$)$_3$ formed from the reaction of Ti(NMe$_2$)$_4$ and SiH$_4$ are essential for Si$_3$N$_4$ growth.

It is not clear why the reaction of Ti(NMe$_2$)$_4$ with SiH$_4$ is not complete, yielding the black solids containing unreacted −NMe$_2$ ligands. The observations of equilibria in the reactions of an amide ligand in (Me$_2$N)$_3$ZrSi(SiMe$_3$)$_3$ (**5**) with silanes to give Zr−H in **6** and aminosilanes (Scheme 3-I) suggest similar *reversible* reactions may occur in the reaction of Ti(NMe$_2$)$_4$ with SiH$_4$ (Scheme 4). These *reversible* reactions perhaps contribute in part to the presence of unreacted −NMe$_2$ ligands in the black solid products.

Acknowledgment is made to the National Science Foundation [CHE-9904338 and NSF Young Investigator program CHE-9457368 (Z.X.), and CHE-9628768 for the purchase of a CCD-based diffractometer at the University of Delaware (A.L.R.)], DuPont Young Professor program (Z.X.), Camille Dreyfus Teacher-Scholar program (Z.X.), Ziegler Research Fund (Z.X.), U.S. Department of Energy under contract DE-AC05-00OR22725 with the Oak Ridge National Laboratory, managed by UT-Battelle, LLC (D.B.B., C.E.V., and R.A.Z.), the Research Grant Council of Hong Kong (Y.D.W.), and Croucher Senior Research Fellowship program (Y.D.W.) for support of this research. We also thank Dr. Albert A. Tuiman for help with mass spectroscopy experiments, Professors David C. Joy and Zheng Xu for EDS and XPS analyses of the powder samples, and Professor Robert G. Bergman for sharing results before their publication.

Supporting Information Available: Further characterization of film **9**, packing diagrams of **1** and **2**, variable-temperature ^{1}H NMR spectra of **1**, XPS of film **9**, SEM of film **9**, schemes of hot-wall horizontal CVD apparatus and a static reaction tube for the reactions of M(NMe$_2$)$_4$ with SiH$_4$, and a complete list of the crystallographic data for **1** and **2** (PDF). This material is available free of charge via the Internet at http://pubs.acs.org.

JA010744S

(57) (a) Aoki, T.; Ogishima, T.; Wrobel, A. M.; Nakanishi, Y.; Hatanaka, Y. *Vacuum* **1998**, *51*, 747. (b) Yasui, K.; Otsuki, K.; Akahane, T. *J. Non-Cryst. Solids* **1994**, *169*, 301. (c) Boudreau, M.; Boumerzoug, M.; Mascher, P.; Jessop, P. E. *Appl. Phys. Lett.* **1993**, *63*, 3014. (d) Gordon, R. G.; Hoffman, D. M.; Riaz, U. *Chem. Mater.* **1990**, *2*, 480.

(58) Habraken, F. H. P. M.; Kuiper, A. E. T.; Van Oostrom, A.; Tamminga, Y.; Theeten, J. B. *J. Appl. Phys.* **1982**, *53*, 404.